Bioactive Materials 8 (2022) 449–477

Contents lists available at ScienceDirect

Bioactive Materials

journal homepage: www.sciencedirect.com/journal/bioactive-materials

Photothermal scaffolds/surfaces for regulation of cell behaviors

Yangcui Qu [a,1], Kunyan Lu [d,1], Yanjun Zheng [d], Chaobo Huang [b], Guannan Wang [a,**], Yanxia Zhang [c,***], Qian Yu [d,*]

[a] College of Biomedical Engineering & the Key Laboratory for Medical Functional Nanomaterials, Jining Medical University, Jining, 272067, PR China
[b] Joint Laboratory of Advanced Biomedical Materials (NFU-UGent), College of Chemical Engineering, Nanjing Forestry University, Nanjing, 210037, PR China
[c] Department of Cardiovascular Surgery of the First Affiliated Hospital & Institute for Cardiovascular Science, Soochow University, Suzhou, 215006, PR China
[d] State and Local Joint Engineering Laboratory for Novel Functional Polymeric Materials, College of Chemistry, Chemical Engineering and Materials Science, Soochow University, Suzhou, 215123, PR China

ARTICLE INFO

Keywords:
Photothermal scaffolds
Photothermal surfaces
Tumor ablation
Intracellular delivery
Cell detachment

ABSTRACT

Regulation of cell behaviors and even cell fates is of great significance in diverse biomedical applications such as cancer treatment, cell-based therapy, and tissue engineering. During the past decades, diverse methods have been developed to regulate cell behaviors such as applying external stimuli, delivering exogenous molecules into cell interior and changing the physicochemical properties of the substrates where cells adhere. Photothermal scaffolds/surfaces refer to a kind of materials embedded or coated with photothermal agents that can absorb light with proper wavelength (usually in near infrared region) and convert light energy to heat; the generated heat shows great potential for regulation of cell behaviors in different ways. In the current review, we summarize the recent research progress, especially over the past decade, of using photothermal scaffolds/surfaces to regulate cell behaviors, which could be further categorized into three types: (i) killing the tumor cells via hyperthermia or thermal ablation, (ii) engineering cells by intracellular delivery of exogenous molecules via photothermal poration of cell membranes, and (iii) releasing a single cell or an intact cell sheet via modulation of surface physicochemical properties in response to heat. In the end, challenges and perspectives in these areas are commented.

1. Introduction

Regulation of cell behaviors (e. g. adhesion, migration, and proliferation) and even cell fates (e. g. differentiation and apoptosis) is of great significance in diverse biomedical applications such as cancer treatment, cell-based therapy, and tissue engineering [1,2]. During the past decades, various methods have been developed including application of external stimuli (e. g. magnetic field, electricity, and stress/-strain), delivering exogenous molecules (e. g. genes and functional proteins) into cell interior and changing the physicochemical properties (e. g. hardness, morphology, and chemical composition) of the substrates where cells adhere to regulate cell behaviors including promotion of cell death to ablate tumors, facilitation of transfection of desired genes for disease diagnosis and cell-based therapy, and stimulation of directional differentiation of stem cells and harvest of cell sheets for tissue engineering [3–6].

Thermal stimulus is a versatile and convenient factor for regulation of cell behaviors because many substances in cells are sensitive to heat and temperature is easily to be controlled on-demand [7]. In general, the heat can affect cell behaviors directly or indirectly. On the one hand, intensive heat can cause protein unfolding and aggregation, DNA damage and irreversible protein denaturation, inducing the damage and even death of cells [8,9]. Moreover, proper heat can enhance the permeability of cell membranes without compromising cell viability, facilitating the entry of functional materials or biomacromolecules into cytoplasm for “engineering” cells [10,11]. On the other hand, the heat can change the physicochemical properties of substrates where cells adhere to affect the cell-surface interactions, modulating the cell

Peer review under responsibility of KeAi Communications Co., Ltd.
* Corresponding author.
** Corresponding author.
*** Corresponding author.
E-mail addresses: chemwangguannan@gmail.com (G. Wang), zhangyanxia@suda.edu.cn (Y. Zhang), yuqian@suda.edu.cn (Q. Yu).
[1] Y. Q. and K. L. contributed equally.

https://doi.org/10.1016/j.bioactmat.2021.05.052
Received 23 April 2021; Received in revised form 18 May 2021; Accepted 31 May 2021
Available online 10 June 2021

behaviors on the surface [12].

Photothermal scaffolds/surfaces refer to a kind of materials embedded or coated with photothermal agents (PTAs, e. g. noble metal nanomaterials, semiconductor nanomaterials, carbon-based nanomaterials, and conjugated polymers) [13–16] that can absorb light with proper wavelength (usually in near infrared (NIR) region) and convert light energy to thermal energy, showing great potential for regulation of cell behaviors in different ways as mentioned above. Specifically, in this review the photothermal scaffolds are based on materials with a specific spatial structure that can embed/wrap PTAs and other functional cargoes (e.g. chemical drugs and photosensitizers) inside the interior of materials. Currently, there are various methods for preparation of scaffolds including conventional methods (e.g. solvent casting, particulate leaching, melting molding, gas foaming, thermally induced phase separation and freeze drying technique) and advanced techniques such as (e.g. electrospinning, rapid prototyping (also known as 3D printing technique) and 4D bioprinting) [17,18]. The photothermal surfaces are generally fabricated by firm immobilization/deposition of PTAs on the surfaces or directly made of materials with photothermal effect. One of the remarkable advantages of the photothermal scaffolds/surfaces is the capability to precise control the heat in space, time, and intensity by changing the conditions of light irradiation because the heat is converted from light. Moreover, NIR light with a wavelength range of 700–1400 nm has the ability to penetrate tissues with low light attenuation and slight damage [19].

In this review, we summarize the recent progress of research, especially over the past decade, on using photothermal scaffolds/surfaces to regulate cell behaviors, which are further discussed under three headings: (i) photothermal scaffolds for killing tumor cells via hyperthermia or thermal ablation (Section 2); (ii) photothermal scaffolds/surfaces for engineering cells by intracellular delivery of exogenous molecules via photothermal poration of cell membranes (Section 3) and (iii) photothermal surfaces for releasing a single cell or an intact cell sheet via modulation of surface physicochemical properties in response to heat (Section 4) as illustrated in Scheme 1. Additionally, besides photothermal scaffolds/surfaces for regulating mammalian cell behaviors, there are also considerable reports on such scaffolds/surfaces for regulating bacterial behaviors, in particular, killing pathogenic bacteria. These reports are summarized comprehensively in other recent reviews [20–23]. Last, a brief comment on the current challenges and perspectives is provided.

2. Photothermal scaffolds for tumor ablation

Cancer is one of the most serious threats to human health. Currently, there are mainly three strategies for cancer treatment including surgical resection, chemotherapy, and radiotherapy [24–26], which, however, still have some limitations such as side effects, cancer palindromia, and reduction of the life quality of patient. In recent years, photothermal therapy (PTT) that relies on hyperthermia generated by PTAs from light energy to thermally ablate tumor cells has nowadays attracted considerable attentions. Compare with conventional therapeutic methods, the main advantages of PTT include the ability to penetrate deep tissue and slight side effects of healthy cells that are not selected [27,28]. So far, a variety of nanomaterial-based PTAs (e.g. gold nanoparticles (GNPs), gold nanorods (GNRs), graphene oxide (GO), polydopamine nanoparticles (PDA NPs) and black phosphorus (BP), etc.) have been utilized for tumor ablation [29]. Although these nano-PTAs show good therapeutic effects, they may accumulate in metabolic organs under a long period, leading to tissue toxicity and inflammatory reactions [30,31]. Photothermal scaffolds refer to the scaffolds embedded/loaded with PTAs and thus own the capability to convert the absorbed light energy into heat, which may trigger some hazardous effects such as lysis of cell membrane, aggregation and denaturation of proteins, and evaporation of cytosol, thereby leading to the death of tumor cells. Compared to nano-PTAs, photothermal scaffolds show extra advantages including controlled heat generation, local ablation on tumor sites, and improved biocompatibility. Moreover, together with PTAs, chemical drugs or photodynamic reagents can also be loaded/embedded in the photothermal scaffolds to realize synergistic anti-tumor effects via the combination of PTT/chemotherapy or PTT/photodynamic therapy (PDT). To the best of our knowledge, photothermal scaffolds applied to cancer therapy mainly include hydrogels, electrospun fibers and 3D printing porous scaffolds. Hydrogels are usually prepared through freeze drying method, spraying or mixing method, showing 3D porous structure and being capable of holding large amounts of water. Electrospun fibers are fabricated through electrospinning technique; the high surface area, high porosity and cross-linked porous structure of such fibers are highly

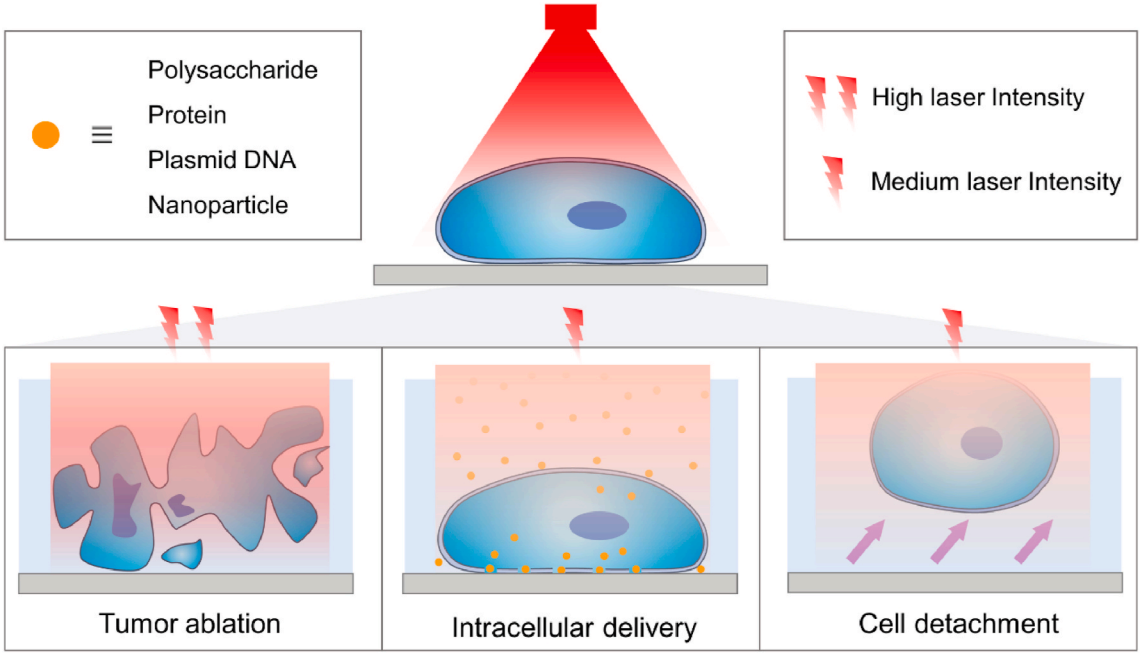

Scheme 1. Three types of photothermal scaffolds/surfaces for regulating cell behaviors under proper NIR irradiation.

similar to tissues and organs. 3D printing porous scaffolds are fabricated through 3D-printing technique that constructs a scaffold by printing layer-by-layer with precise control of macro-nano structures. In **Section 2**, the development of photothermal scaffolds for tumor ablation are introduced and categorized into three classes: (i) hydrogel-based, (ii) electrospun fiber-based, and (iii) 3D (three-dimensional) printing porous scaffold-based (Table 1).

2.1. Hydrogel-based photothermal scaffolds

Hydrogel is a family of soft matters that has 3D networks of cross-linked hydrophilic polymer chains [67]. Hydrogels are ideal candidates for cancer treatment because they are generally biocompatible and can be loaded/embedded with a series of functional molecules such as drugs and deliver them to targeted sites [68,69]. In recent years, several photothermal hydrogels were fabricated by incorporation of PTAs (e.g. GNPs [33], Fe_3O_4 NPs [34], PDA NPs [38], poly (diketopyrrolopyrrole-alt-3,4-ethylenedioxythiophene) (PDPPEDOT) NPs [39], GO sheets [43]) for eradication of tumor cells and ablation of solid tumors.

In general, the tumor cells can be ablated by the heat directly produced by hydrogel-embedded PTAs under NIR irradiation with proper intensity. For example, Chen and co-workers prepared several gelatin (a natural biopolymer deriving from collagen)-based hydrogels containing different PTAs including GNRs, gold nanostars (GNSTs) and Fe_3O_4 NPs by freeze-drying method, achieving ablation of HeLa cells in vitro [32–35]. As shown in Fig. 1a, HeLa cells attached to the gelatin/GNPs composite hydrogel were eradicated by the hyperthermia under 805 nm NIR irradiation [33]. In the following work, in order to achieve the targeted tumor ablation, they introduced folic acid (recognizing folate receptors (FR-α, β, γ) overexpressed in tumor cells [70]) on the surface of composite hydrogels to selectively capture of HeLa cells for further thermal ablation. Compared to the photothermal hydrogel without folic acid modification, the folic acid-modified photothermal hydrogel promoted cell adhesion on surface of hydrogel, improving the killing efficiency correspondingly [34]. They also found that the tumor cells killed by hyperthermia could promote the activation and maturity of dendritic cells, which was expected to activate the immune system to inhibit the metastasis and recurrence of tumors (Fig. 1b) [35].

Common PTT generally requires high temperature (>50 °C) to effectively ablate the tumor cells, however, such high temperature will lead to collateral damage to nearby healthy cells and normal tissues and induce inflammatory diseases by the indiscriminate heating inevitably. Low-temperature (<45 °C) PTT as a clear term has recently emerged to circumvent this problem [71], however, so far, such strategy has not been applied to photothermal scaffolds for tumor therapy. Alternatively, multi-model therapy (e.g. PTT/chemotherapy, PTT/PDT) have been developed to improve the ability of tumor ablation and decrease the laser intensity for PTT. Some anticancer drugs were incorporated into the hydrogels together with PTAs to generate a synergistic anti-tumor effect via the combination of chemotherapy and PTT. For example, Cheng and co-workers immobilized SN38 as anticancer drug on PDA NPs via strong π-π stacking interaction, and incorporated the complexes into a PEG hydrogel [37]. Under NIR irradiation, the generated heat from PDA NPs weaken the π-π stacking interaction to trigger the release of SN38, showing improved ablation efficiency to inhibit the growth of mouse PC-9 tumors in vivo [72]. To better realize the controlled release of drugs in hydrogels, stimulus-responsive hydrogels, in particular, temperature responsive poly (N-isopropylacrylamide) (PNIPAAm)-based hydrogels were chosen as the matrixes. As shown in Fig. 2a, Kim and co-workers developed a dual-responsive composite hydrogel based on a PNIPAAm hydrogel embedded with an anticancer drug DOXO together with PDA NPs loaded with bortezomib (BTZ, another anticancer drug) via the formation of borate bonds between the boronic acid groups of BTZ and catechol groups of PDA [38]. Under NIR irradiation, the produced heat ablated tumor cells and caused the shrinking of hydrogel to release DOXO (Fig. 2b). Moreover, in response to the acidic tumor microenvironment [73], BTZ was released from the surface of PDA NPs due to the dissociation of borate bonds (Fig. 2c). This platform achieved controlled multidrug release and exhibited good thermal ablation ability, showing a super synergistic effect for the tumor treatment. In addition to the combination of PTT and chemotherapy, the combination of PTT and PDT is also an effective method for tumor therapy with improved efficiency. PDT is a non-destructive method that relies on photosensitizer to generate cytotoxic reactive oxygen species (ROS), causing rapid lipid oxidation, protein and DNA damage to kill tumors [74]. The cooperation between PDT and PTT is considered a breakthrough strategy that can overcome their respective shortcomings as PTT can improve the oxygen supply of tumor tissues by increasing blood flow, thereby promoting the PDT effect and reducing the temperature required for PTT [30,75]. For example, Wu and co-workers developed a thermo-responsive chitosan-based hydrogel incorporated with nanosized black titania (B-TiO_{2-x}) nanoparticles showing a crystalline/amorphous core-shell structure with abundant oxygen vacancies, achieving the antitumor performance by simultaneous PTT/PDT effects [41]. Under a single-wavelength NIR irradiation, the B-TiO_{2-x} nanoparticles converted the light energy into heat and generated cytotoxic ROS to kill cutaneous tumor cells in vitro and inhibit tumor growth in vivo.

So far, surgical resection remains the preferred method of treatment of skin cancer, bone cancer and breast cancer [76]. However, after surgical removal of the tumor, there are two possible residual problems: (i) if the tumor tissue is not completely removed, the remaining tumor cells would continue proliferation and metastasis, and (ii) the large area tissue defects caused by surgical resection are hard to recover [77]. It is thus promising to construct a bifunctional material that is able to eliminate tumor and promote tissue regeneration simultaneously. In this regard, a series of bioactive components with capability to promote the regeneration of defective tissues were incorporated into photothermal hydrogels [42–44]. For example, He, Yu and co-workers constructed a stable hydrogel *via* the self-assemble of two functional materials including reduced graphene oxide (rGO) and nano-hydroxyapatite (nHA) [43]. rGO not only has good photothermal property but also can induce the differentiation of bone marrow stem cells (BMSCs) into osteoblasts and promote bone repair in vivo [78]; nHA is widely used as artificial bone to repair bone defects because it can promote the osteogenic differentiation of rBMSC [79]. Under NIR irradiation, this composite hydrogel ablated osteosarcoma cells (MG-63) effectively in vitro and prevented tumor growth in vivo. After the implantation the hydrogel in the bone defect of rabbit, dense new bone tissue was observed on the cross-section of the entire scaffold after eight weeks (Fig. 3a), indicating good osteogenic ability of the hydrogel. In addition to the treatment of breast cancer and bone cancer, hydrogels have more extensive applications in skin cancer and melanoma because the permeable structure is favorable for adsorption of wound exudate and exchange of gas, thus promoting wound regeneration and angiogenesis [80]. To this end, Wu and co-workers developed a smart oligomeric proanthocyanidins (OPC, deriving from grape seed extract)-containing hydrogel to cure melanoma and promote wound healing (Fig. 3) [44]. In this design, OPC was not only used as a natural photothermal agent, but also facilitated wound healing. Under NIR irradiation, the composite hydrogel effectively killed melanoma cells and inhibited tumor growth. Moreover, it also promoted the migration and proliferation of skin fibroblast and endothelial cells, thereby facilitating the angiogenesis and skin regeneration. Although hydrogels are easy to prepare and have been widely used in PTT, they still have some disadvantages. For example, most of the hydrogels are prepared through freeze drying and simple mixing methods, making it difficult to control the structure, diameter of the pores and the porosity of the scaffolds. Moreover, due to the low mechanical strength and fragile nature of the hydrogels, the feasibility of applying hydrogels is still limited.

Table 1
Summary of photothermal scaffolds for tumor ablation [a].

PTAs	Light wavelength	Functional molecules	Matrix materials	Preparation methods	Performance of scaffolds	Cell Line	Ref.
Hydrogel-based photothermal scaffolds							
Fe3O4 NPs	805 nm	N. A.	Gelatin	Ice particulate porogen method	Cancer cell entrapment + PTT	HeLa cells in vitro	[32]
GNRs/GNSTs	805 nm	N. A.	Gelatin	Ice particulate porogen method	Cancer cell entrapment + PTT	HeLa cells in vitro	[33]
Fe_3O_4 NPs	805 nm	Folic acid	Gelatin/PLL	Ice particulate porogen method	Cell capture + PTT	HeLa cells in vitro	[34]
GNRs	805 nm	N. A.	Gelatin	Ice particulate porogen method	Cancer cell entrapment + PTT + Immune activation	4T1-Luc cells in vitro; mDCs	[35]
BP	808 nm	N. A.	PLEL	Spraying method	PTT	MB231-Luc cells tumor-bearing mice in vivo	[36]
PDA NPs	808 nm	SN38	PEG	Mixing method via Michael addition and/or Schiff base reactions	Chemotherapy + PTT	mouse PC-9 cells	[37]
PDA NPs	808 nm	DOXO/BTZ	P(NIPAAm-co-AAm)	Radical polymerization and mixing method	Chemotherapy + PTT	CT26 colon cancer cells in vitro	[38]
PDPPEDOT	808 nm	DOX	PNIPAAm	Radical polymerization and spin-coating method	Chemotherapy + PTT	HeLa cells	[39]
GO	808 nm	DOX	CSMA/BPEI/BPEI-GO	Mixing method	Self-healing + Chemotherapy + PTT	MCF-7 cells in vitro; Mice bearing 4T1 cells in vivo	[40]
Black titania	808 nm	Black titania	Chitosan	Mixing method	PTT + PDT + Tissue regeneration	B16F10 cells in vitro; Mice bearing B16F10 cells in vivo; HDFs; HUVECs	[41]
GNRs	805 nm	N. A.	Gelatin	Ice particulate porogen method	PTT + Tissue regeneration	MDA-MB231-Luc cells in vitro; MDA-MB231-Luc cells tumor-bearing mice in vivo hMSCs for tissue regeneration	[42]
rGO	808 nm	nHA	nHA-rGO	Simply mixing method and *in situ* self-assembly	PTT + Bone regeneration	MG-63 cells; rBMSCs	[43]
OPC	N.A.	N. A.	Calcium silicate nanowires and sodium alginate (CS-SA)	3D-printing technology	PTT + Would healing	B16F10 cells in vitro; Mice bearing B16F10 tumor in vivo; HUVECs/HDFs	[44]
Electrospun fiber-based photothermal scaffolds							
Bi_2Se_3	808 nm	N. A.	PLLA	Electrospinning	PTT	HeLa, HSF cells in vitro, solid tumor in vivo	[45]
GO	810 nm	GO	PCL	Electrospinning	Cell capture + PTT	MCF-7 cells	[46]
Cu_9S_5	980 nm	N. A.	PCL/gelatin	Electrospinning	Chemotherapy + PTT	HeLa cells in vitro; H22 cells tumor in vivo	[47]
PDA NPs	808 nm	BTZ	Polydioxanone	Electrospinning	Biodegradability + Chemotherapy + PTT	CT26 cells in vitro	[48]
PPy	808 nm	PTX/PPy	PCL	Electrospinning	Control of drug release + Chemotherapy + PTT	CT26/MCF7 cells in vitro; MCF7 tumor in vivo	[49]
PDA NPs	808 nm	DOX for chemotherapy	PCL	Electrospinning	Control of drug release + Chemotherapy + PTT	A549/MCF7 cells in vitro	[50]
PDA NPs	808 nm	DOX for chemotherapy	PCL-Gelatin fiber	Electrospinning	Control of drug release + Chemotherapy + PTT	CCLP1 cells in vitro; PDX model in vivo	[51]
Cu_2S	808 nm	Cu ions for accelerating tissue healing	PLA/PCL	Patterning coelectrospinning	PTT + Tissue regeneration	B16F10/A375melanoma cells in vitro; B16F10 tumor-bearing mice in vivo; HDFs	[52]
$CaCuSi_4O_{10}$NPs	N.A.	Cu^{2+} and SiO_4^{4-} ions for accelerating tissue healing	PCL/PDLLA	N. A.	PTT + Tissue regeneration	B16F10 cells in vitro; B16F10 tumor-bearing mice in vivo	[53]
CSO HMSs	808 nm	Trametinib for chemotherapy, Cu ions and silicate-based biomaterials for accelerating tissue healing	PLA/PCL	Electrospinning	Chemotherapy + PTT + Tissue regeneration	B16F10 cells in vitro; B16F10 tumor-bearing mice in vivo	[54]
3D printing porous scaffold-based photothermal scaffolds							
GO	808 nm	N. A.	β-TCP	3D-printing and surface modification technology	PTT + Bone regeneration	MG-63 cells in vitro; Saos-2 tumor-bearing mice in vivo; rBMSCs in vitro	[55]
PDA	808 nm		Bioceramic	3D-printing and surface self-assembly	PTT + Bone regeneration	Saos2/MDA-MB-231 cells in vitro; Saos2 tumor-bearing	[56]

(*continued on next page*)

Table 1 (*continued*)

PTAs	Light wavelength	Functional molecules	Matrix materials	Preparation methods	Performance of scaffolds	Cell Line	Ref.
		Ca and P elements for promoting bone generation				mice in vivo; rBMSCs in vitro; Critical-sized femoral defect model in vivo	
MoS_2	808 nm	N. A.	Akermanite (AKT) bioceramic	3D-printing and hydrothermal method	PTT + Bone regeneration	Saos2/MDA-MB-231 cells in vitro; Saos2 tumor-bearing mice in vivo; rBMSCs in vitro; Critical-sized femoral defect model in vivo	[57]
MoS_2	808 nm	N. A.	Bioactive glass	3D-pringitng and spin-coating method	PTT + Bone regeneration	MNNG/HOS Cells in vitro; MNNG/HOS tumor-bearing mice in vivo; rBMSCs in vitro; critical-sized rat calvarial defects	[58]
Free carbons	808 nm	Free carbon and larnite for enhancing osteogenic differentiatio	Larnite	3D printing and polymer-derived ceramics strategy	PTT + Bone regeneration	MNNG/HOS cells in vitro; HOS tumor-bearing mice in vivo; rBMSCs; critical-sized rat calvarial defects	[59]
Fe	808 nm	N. A.	AKT bioceramic	Sol-gel and 3D-printing technology	PTT + MTT + Osteogenic differentiation	LM-8 cells, rBMSCs	[60]
Nb_2C nanosheets	1064 nm	2D Nb_2C nanosheets wrapped with S-nitrosothiol for providing NO	Bioactive glass	Solution-soaking approach and 3D-printing technology	PTT + NO therapy + Bone regeneration	Saos2 cells; Saos2 tumor-bearing mice in vivo; hBMSCs; critical-sized rat calvarial defects	[61]
BP	808 nm	N. A.	Bioactive glass	3D-printing and surface modification method	PTT + Bone regeneration	Saos2 cells in vitro; Saos2 tumor-bearing mice in vivo; hBMSCs in vitro; critical-sized rat calvarial defects	[62]
Ti_3C_2 nanosheets	808 nm	Ca^{2+}, PO_4^{3+} and Ti-based species for promoting bone regeneration	Bioactive glass	3D-printing and soak-coating method	PTT + Bone regeneration	Saos2 cells; Saos2 tumor-bearing mice in vivo; hBMSCs; critical-sized rat calvarial defects	[63]
$CuFeSe_2$ nanocrystals	808 nm	N. A.	Bioactive glass	3D printing technique with solvothermal method	PTT + Bone regeneration	Saos2 cells in vitro; Saos2 tumor-bearing mice in vivo; rBMSCs in vitro; Critical-sized femoral defect model in vivo	[64]
Cu, Fe, Mn, Co	808 nm	N. A.	Bioactive glass-ceramic	3D-printing technology	PTT + Bone regeneration	Saos2 cells in vitro; Saos2 tumor-bearing mice in vivo; rBMSCs in vitro	[65]
LaB_6 micro-NPs	808 nm	N. A.	β-TCP	3D-printing and soak-coating method	PTT + Bone regeneration	Saos2 cells in vitro; Saos2 tumor-bearing mice in vivo; rBMSCs in vitro;Critical-sized femoral defect model in vivo	[66]

[a] Abbreviation: Reduced graphene oxide (rGO); Gold nanostars (GNSTs); Copper silicate hollow microspheres (CSO HMSs); Oligomeric proanthocyanidins (OPC); doxorubicin (DOX); Bortezomib (BTZ); Paclitaxel (PTX); Poly-L-lysine (PLL); Polyvinyl alcohol (PLA); Polyethylene glycol (PEG); Poly(L-lactic acid) (PLLA); Polycaprolactone (PCL); Poly(D, L-lactic acid) (PDLLA); Polypyrrole (PPy); Human umbilical vein endothelial cells (HUVECs); Human skin fibroblast (HSF); Rat bone marrow stem cells (rBMSCs);human bone marrow stem cells (hBMSCs); Human dermal fibroblasts (HDFs); patient-derived xenograft (PDX); Poly (N-isopropylacrylamide) (PNIPAAm); nano-hydroxyapatite (nHA); Poly(diketopyrrolopyrrole-alt-3,4-ethylenedioxythiophene) (PDPPEDOT); Poly(d,L-lactide)-poly (ethylene glycol)-poly(d,L-lactide) (PLEL); Chondroitin sulfate multialdehyde (CSMA), Branched polyethylenimine (BPEI); BPEI conjugated graphene (BPEI-GO);β-tricalcium phosphate (β-TCP).

2.2. Electrospun fiber-based photothermal scaffolds

Electrospun fibers fabricated through electrospinning with polymers have various advantages including high specific surface area, adjustable nano/micro structure, and ability for loading functional molecules such as drugs, growth factors, etc. Therefore, they have attracted wide attention as implantable materials for treatment of solid tumors [81–83]. Photothermal electrospun fibers are constructed by embedding PTAs into interior of fibers or coating PTAs on the surface of fibers. In recent years, various natural polymers and synthetic polymers have been applied to fabricate photothermal electrospun fibers for tumor ablation.

Yu and co-workers prepared poly(L-lactic acid) (PLLA)-based electrospun fibers containing Bi_2Se_3 through uniaxial electrospinning technology, which achieved efficient ablation of HeLa cells under NIR irradiation. In addition, the tumor surgically incised and covered with Bi_2Se_3/PLLA fiber was getting smaller, compared to that without fiber coverage or with PLLA fiber coverage [45]. Although these fibers exhibited good efficiency of tumor ablation, the hyperthermia might result in certain harmful effects on normal cells and tissues. In order to decrease the temperature for killing tumor cells, a series of multifunctional electrospun fibers combining PTT and other therapeutic methods were developed [84,85]. For example, Lin, Li and co-workers incorporated core-shell Cu_9S_5@mesoporous SiO_2 nanoparticles embedded with DOX in electrospun fiber membranes composed of polycaprolactone (PCL) and gelatin, achieving efficient ablation of hepatoma H22 tumor (Fig. 4a) [47]. Under NIR irradiation, Cu_9S_5 nanoparticles produced heat, which not only achieved thermal ablation of tumor cells, but also promoted the release of DOX, enhancing the therapeutic effects. Afterwards, Kim and co-workers developed a series of electrospun fibers

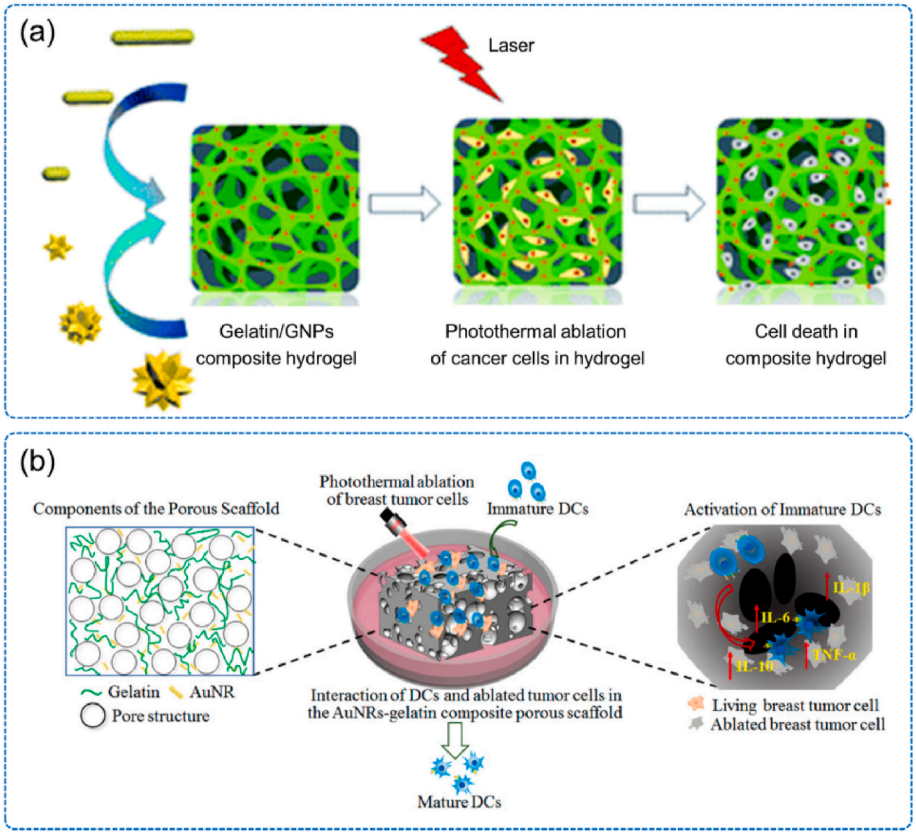

Fig. 1. (a) A composite hydrogel composed of gelatin and GNPs with controllable size and shape for ablation of tumor cells under NIR irradiation. Reproduced with permission from Ref. 33. Copyright 2017 The Royal Society of Chemistry. (b) Interactions between DCs and tumor cells ablated by a photothermal composite scaffold under NIR irradiation. Reproduced with permission from Ref. 35. Copyright 2019 Multidisciplinary Digital Publishing Institute.

wrapped/loaded with chemical drugs and PTAs, achieving excellent ablation of colon cancer cells and breast cancer cells by synergistic effect of chemotherapy and PTT [48–50]. For example, they prepared a composite fiber composed of polydioxanone (PDO) embedded with PDA NPs as PTAs and BTZ as drugs, which could ablate the colon tumor cells in 3-min NIR irradiation due to the released BTZ and induced hyperthermia (Fig. 4b) [48]. In order to further improve the controlled release of chemical drugs, polypyrrole (PPy) with both excellent photothermal properties and pH-responsiveness was coated *in situ* on the surface of PCL-based electrospun fiber embedded with a drug of paclitaxel (PTX). In the acidic environment of tumors [73], the swelling of PPy accelerated the release of PTX. Under NIR irradiation, the PPy coating not only realized the efficient thermal ablation of the tumor, but also accelerated the release of PTX, promoting the therapeutic effect and maintaining good biocompatibility.

Similar to hydrogels as mentioned above, it is also of importance to endow electrospun fibers with capability of both tumor ablation and tissue regeneration. To this end, Wu and co-workers developed a series of such dual-functional electrospun fibers [52–54]. For example, they fabricated micropatterned nanocomposite fibers by incorporating Cu_2S nanoflowers into poly(D,L-lactic acid) (PDLLA)/PCL fibers (CS-PLA/PCL) *via* a modified electrospinning method (Fig. 5a) [52]. Because of good photothermal properties of Cu_2S nanoflowers, under NIR irradiation the resulted fibers ablated skin tumor cells in vitro and prevented tumor growth in vivo effectively. In addition, the released Cu^{2+} ions from CS-PLA/PCL membranes could promote angiogenesis and enhance the maturity of the extracellular matrix (ECM) via regulation of corresponding gene expression [86], thus promoting the adhesion, migration, and proliferation of normal skin cells in vitro (Fig. 5a), and stimulating angiogenesis and heal full-thickness skin defects in vivo. In another work, inspired by the shape of Chinese sesame sticks, they coated the surface of polyvinyl alcohol (PLA)/PCL electrospun fibers with $CaCuSi_4O_{10}$ nanoparticles, showing the similar structure as Chinese sesame sticks (Fig. 5b) [53]. Besides the photothermal tumor ablation property from $CaCuSi_4O_{10}$ nanoparticles, the active Cu^{2+} and SiO^{4-} ions released from the fibers could stimulate angiogenesis and re-epithelialization [87], thereby promoting chronic wound healing. To further enhance ablation efficiency, they fabricated PLA/PCL composite fibers wrapped with anticancer drug (trametinib)-loaded copper silicate hollow microspheres, achieving synergistic chemo-photothermal killing effects of skin tumor cells and facilitating the healing process in tumor-bearing and diabetic mice [54]. Although the electrospinning technology can well control the structure of the fibers and prepare a scaffold with a complex structure (such as random or oriented structures), it should be noted that there are many parameters that need to be adjusted carefully during the preparation process. Moreover, the resulted electrospun fibers are generally two-dimensional (2D) membranes with small pores and low thickness.

2.3. 3D printing porous scaffold-based photothermal scaffolds

Compared with 2D membranes, 3D porous scaffolds may have better effects for tissue regeneration of tumor site *in situ* as the interconnected macropores of 3D porous scaffolds are necessary to supply adequate space for transportation of nutrients communications of neighboring cells [88]. Various methods to prepare 3D porous scaffolds have been developed, among which the 3D printing technology is the preferred option due to its advantages such as easy and economical fabrication of objects, the end-user customization, and rapid prototyping [89–92]. In addition, it is convenient to incorporate bioactive materials during printing process to endow the printing scaffolds desired functions [93]. In the past few years, the introduction of PTAs into the 3D printing

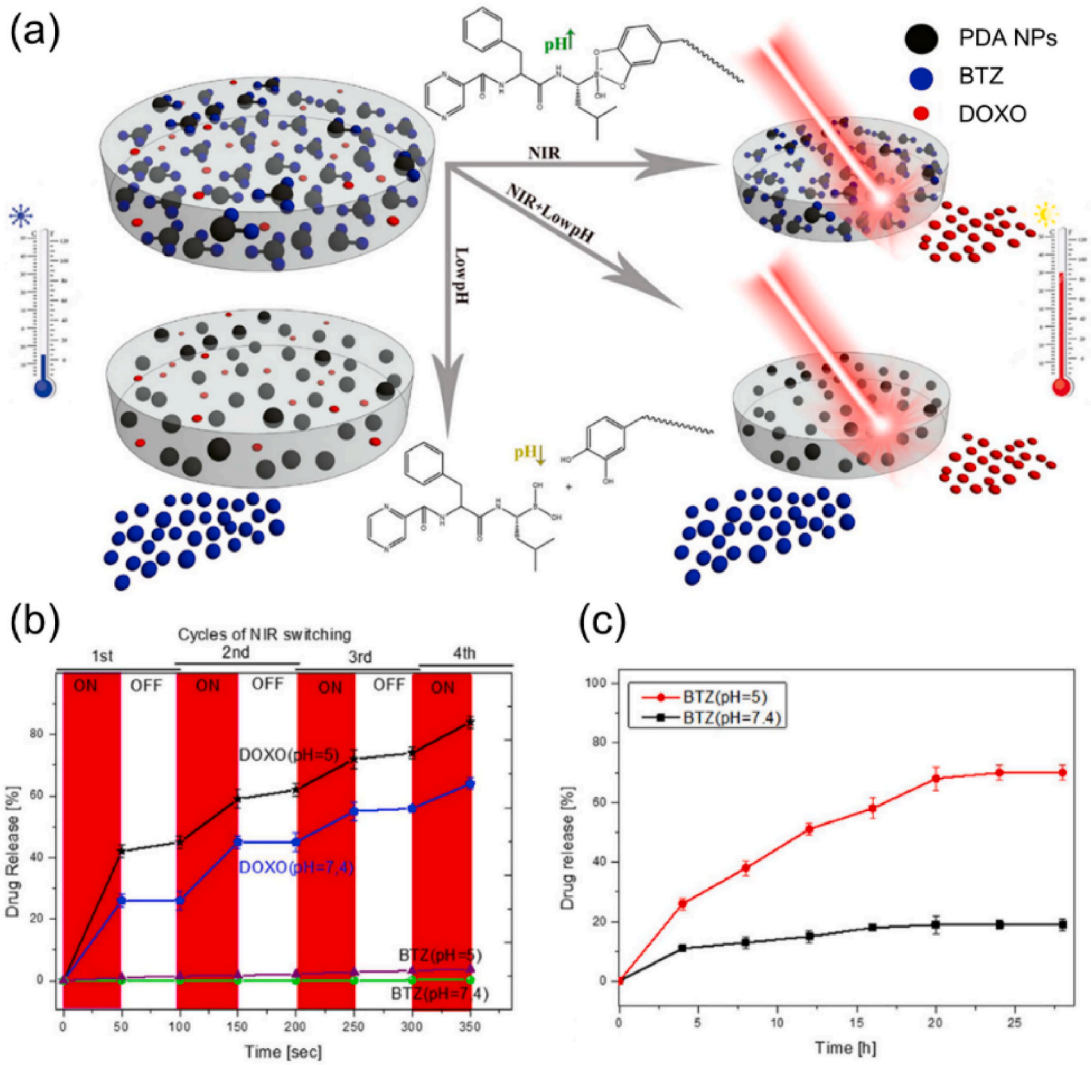

Fig. 2. (a) Scheme of a pH/NIR-dual responsive composite hydrogel for chemo-photothermal cancer therapy. (b) Release profiles of BTZ and DOXO from the composite hydrogel at different pH under cyclic ON/OFF NIR irradiation. (c) Release profile of BTZ from the composite hydrogel at different pH. Reproduced with permission from Ref. 38. Copyright 2016 Springer Nature.

scaffolds to achieve bone tumor ablation and tissue regeneration has attracted increasing attentions [90]. Some representative examples are introduced as follows.

3D printing bioceramic scaffolds have been demonstrated to be able to stimulate osteoblast differentiation, promote angiogenesis in vitro, and initiate bone regeneration in vivo, because the precise interconnected macropores benefit the nutrient transportation and cell ingrowth, and the released bioactive elements (Si, Ca and P) during the scaffold degradation stimulate bone formation and angiogenesis [94]. Based on these advantages, Wu and co-workers developed a series of 3D printing bioceramic scaffolds with excellent photothermal properties, achieving osteoma ablation and bone regeneration effectively [55–57, 60,65,66]. For example, they fabricated a bifunctional GO-modified β-tricalcium phosphate (β-TCP) (GO-TCP) scaffold (Fig. 6a). Under NIR irradiation, the resulted scaffold could ablate >90% of osteosarcoma cells in vitro, and prevent tumor growth in mice effectively. Additionally, the scaffold could stimulate the osteogenic differentiation of BMSCs by up-regulating the expression of bone-related genes, and thus promote bone formation in rabbit bone defects [55]. Afterwards, they introduced PDA coating and MoS_2 nanosheets with better biocompatibility as PTAs onto/into the bioceramic scaffold, respectively, which also achieved photothermal ablation of osteoma and promoted bone regeneration [56,57].

The fabrication method mentioned above involved several steps and might cause the damage of scaffolds to some degree. Aiming at simplification of the preparation process, 3D printing technique was combined with polymer-derived ceramics (PDCs) strategy [95]. For example, Zhao and co-workers developed a larnite scaffold embedded with free carbon (larnite/C) that was fabricated by 3D printing a homogeneous mixture of $CaCO_3$ active filler powders and polysilsesquioxane silicone (Fig. 6b) [59]. The carbon atoms in the organic silicon polymer were thermally decomposed into free carbon during the ceramic conversion process under an inert atmosphere, thus reducing the number of cracks in ceramic foam. Importantly, larnite is a bioactive ceramic with capability to promote formation of apatite and expression of osteogenic genes [96]. Meanwhile, free carbon with high photothermal conversion efficiency could ablate cancer cells under NIR irradiation (Fig. 6b), giving the resulted scaffold great potential for the treatment of malignant bone tumors.

In order to further enhance the effect of osteoma ablation, various scaffolds combining PTT and other treatment mechanisms such as magnetic therapy or gas therapy were developed [60,61]. For example, Wu and co-workers doped Fe element possessing magnetism into the AKT bioceramic scaffold, achieving the synergistic ablation of bone tumors between PTT and magnetic therapy (Fig. 7a) [60]. Magnetic therapy not only could solve the limitation of the penetration depth of

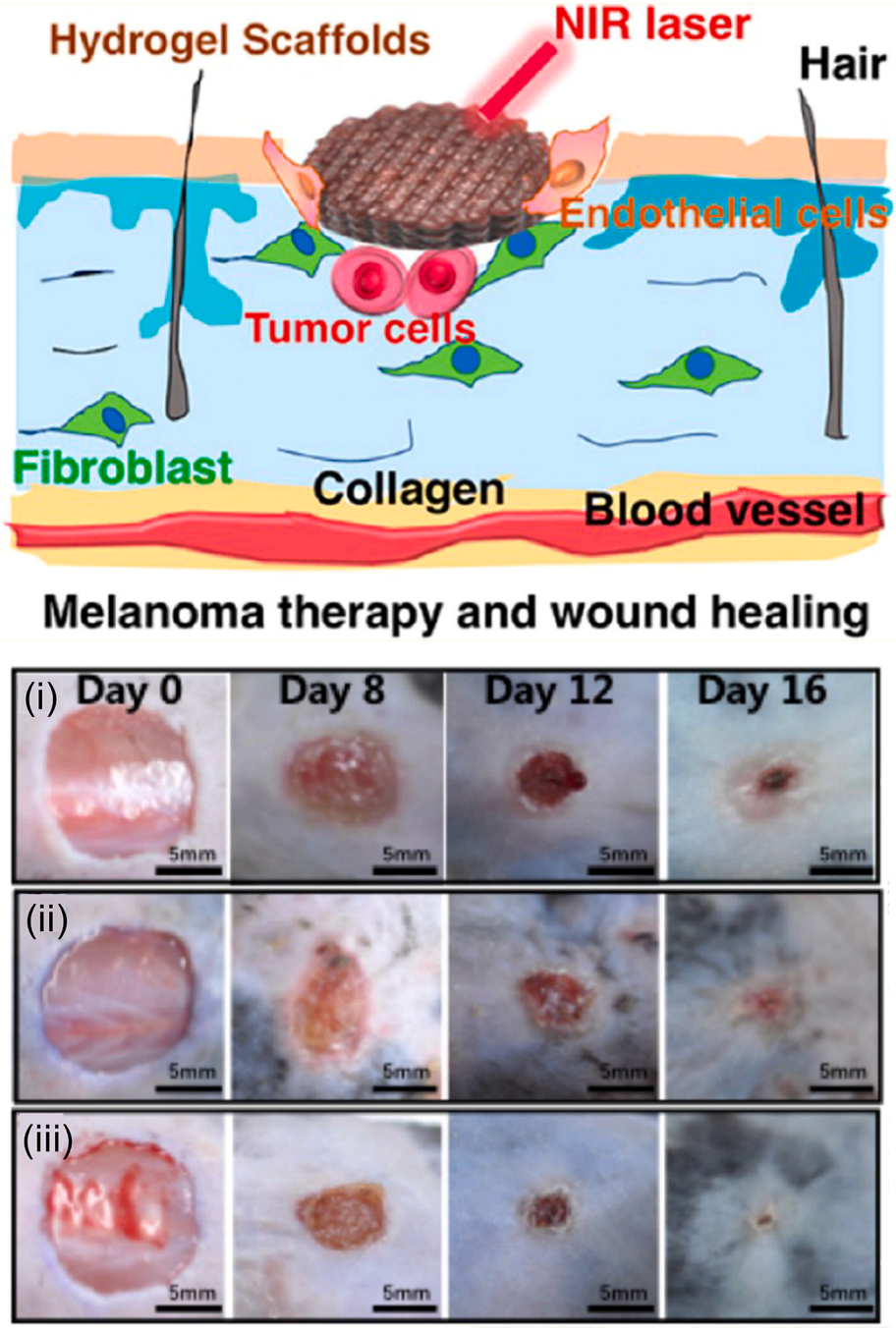

Fig. 3. Top: a composite hydrogel scaffold containing OPC, calcium silicate nanowires (CS) and sodium alginate (SA) for melanoma therapy and wound healing under NIR irradiation; Down: typical photos of skin wounds at different intervals. (i): blank with no treatment, (ii): CS + SA, and (iii) CS + SA + OPC hydrogel scaffold. Reproduced with permission from Ref. 44. Copyright 2019 American Chemical Society.

PTT alone, but also reduce the temperature required for PTT, thereby reducing the damage of excessive temperature to surrounding normal tissues. Cao, Chen, Zhang and co-workers incorporated nitric oxide (NO) donors (S-nitrosothiol, SNO) [97] and mesoporous silicon loaded with MXene nanosheets possessing large specific surface and photothermal property into 3D printing bioglass (BG) scaffold to combine gas therapy and PTT together in one scaffold [61]. In the initial stage, the osteoma cells could be ablated effectively by combining PTT and gas therapy under the action of NO with high concentration. In the later stage, NO with low concentration and BG scaffold could enhance vascularization and bone formation (Fig. 7b), so as to achieve excellent tumor ablation and bone formation.

Most of the PTAs used in the above research only have the ability of ablation of osteoma, but have little effect on osteogenesis. To this end, several bifunctional PTAs possessing abilities of osteoma ablation and enhanced osteogenesis were incorporated into 3D printing scaffolds. For example, Shi and co-workers integrated 2D BP nanosheets on the 3D printing BG scaffold (BP-BG) for photothermal ablation of tumors and osteogenesis [62]. Besides the function of photothermal ablation of tumors in the early stage, BP also enhanced biomineralization *in situ*, thus promoting bone formation under the action of its degradation products. In addition, the oxidation of the BP coating also accelerated the release of phosphate ions (PO_4^{3-}), which could bind the calcium ions from body fluids, thereby promoting the formation of new calcium phosphate

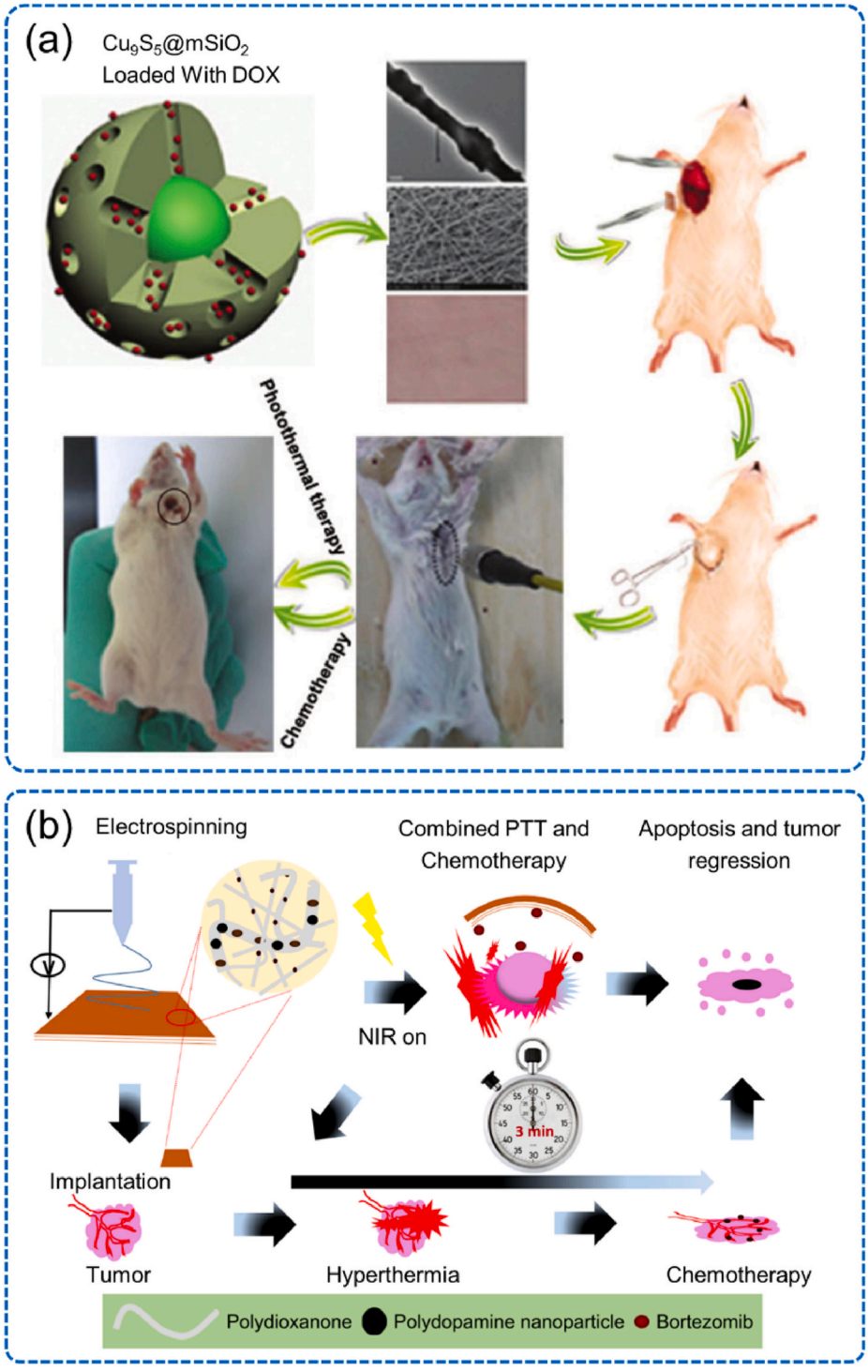

Fig. 4. (a) Schematic illustration of a PCL/gelatin fiber scaffold containing Cu_9S_5@ $mSiO_2$ nanoparticles loaded with DOX for tumor ablation *via* chemotherapy and PTT. Reproduced with permission from Ref. 47. Copyright 2015 The royal society of chemistry. (b) Fabrication of a composite electrospun fiber scaffold composed by polydioxanone, polydopamine nanoparticles and bortezomib for combined photothermal chemotherapy. Reproduced with permission from Ref. 48. Copyright 2018 Dovepress.

nanoparticles (Fig. 8a). Apart from black phosphorus, 2D ultra-thin Ti_3C_2 nanosheets also have such two capabilities of photothermal ability and promoting bone formation [98]. The released Ti-based species in the degradation process by the interaction between water and oxygen could promote the growth of new bones, making Ti_3C_2 nanosheets suitable as dual functional PTAs for fabrication of 3D printing scaffolds to treat bone tumors (Fig. 8b) [63]. The 3D printing technique that can precisely control pore structure of scaffolds has gained strong appeal in the field of tumor treatment. However, the equipment used for 3D printing is expensive and the process takes a relatively long time. Moreover, the types of applicable materials are limited, making it difficult for production in large-scale. In addition to the above three scaffolds including hydrogels, electrospun fibers and 3D printing scaffolds, it is necessary to exploit other photothermal scaffolds integrating simple preparation methods, controllable material structures, and scalable preparation for tumor treatment.

3. Photothermal scaffolds/surfaces for intracellular delivery of exogenous molecules

In addition to generating intensive heat to ablate tumor cells, photothermal scaffolds/surfaces can also produce moderate heat under

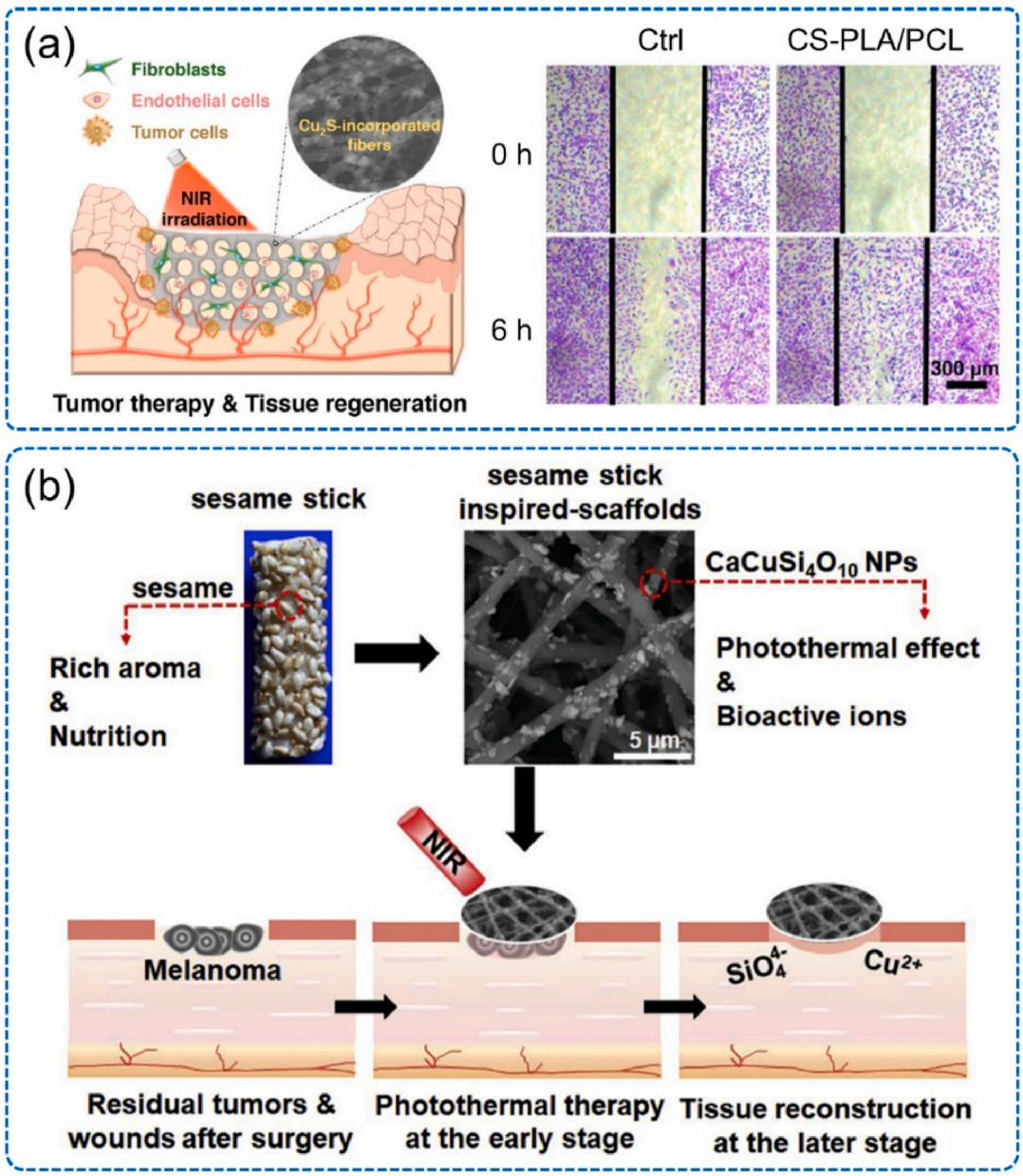

Fig. 5. (a) Left: A CS-PLA/PCL fiber scaffold incorporated with Cu_2S nanoparticles for cancer therapy and tissue regeneration. Right: Results of scratch assay of HUVECs cultured on different sample surfaces. Adapted with permission from Ref. 52. Copyright 2017 American Chemical Society. (b) A sesame stick inspired-scaffold composed of PLA/PCL fibers coated with $CaCuSi_4O_{10}$ nanoparticles for PTT and tissue reconstruction at different stages after surgery. Adapted with permission from Ref. 53. Copyright 2019 Elsevier.

suitable light intensity to increase membrane permeability of cells without obvious cell damage, providing the possibility of intracellular delivery of exogenous molecules. Delivery of exogenous functional materials and biomacromolecules into living cells to regulate their behaviors and fates is a crucial step in cell-based therapy as well as tissue repair and regeneration [99], for example, delivering functional genes into immune cells *ex vivo* to obtain Chimeric Antigen Receptor T (CAR-T) cells for cancer therapy [100] or into adult cells to obtain induce pluripotent stem cells (iPSCs) for tissue regeneration [101]. The plasma membrane of cells, however, is an impermeable barrier for most exogenous molecules [102], and it is still challenging to achieve high delivery efficiency without compromising cell viability. According to the different ways of exogenous molecules passing through the cell membrane, the current intracellular delivery approaches can be categorized into two main classes: carrier-based approaches and membrane disruption-based approaches [103]. Although various carriers such as viral vectors and non-viral vectors including cationic polymers and liposomes have been developed, they still have some limitations including low delivery efficiency, high cell toxicity and limited universality [104]. In contrast, membrane disruption-based approaches transport the exogenous molecules into cells by membrane permeabilization or penetration *via* membrane disruption agents, mechanical, electrical, optical, acoustical, and thermal means, showing broader applications regardless of targeted cell and delivered molecules [105]. Among these membrane disruption-based methods, photothermal-poration has received great interest due to its various advantages including simple equipment, easy operation, and good spatiotemporal control of delivery [106]. In the photothermal-poration method, under NIR irradiation, the heat generated by the PTAs increases the temperature of surrounding medium or generates shock waves or water vapor nanobubbles,

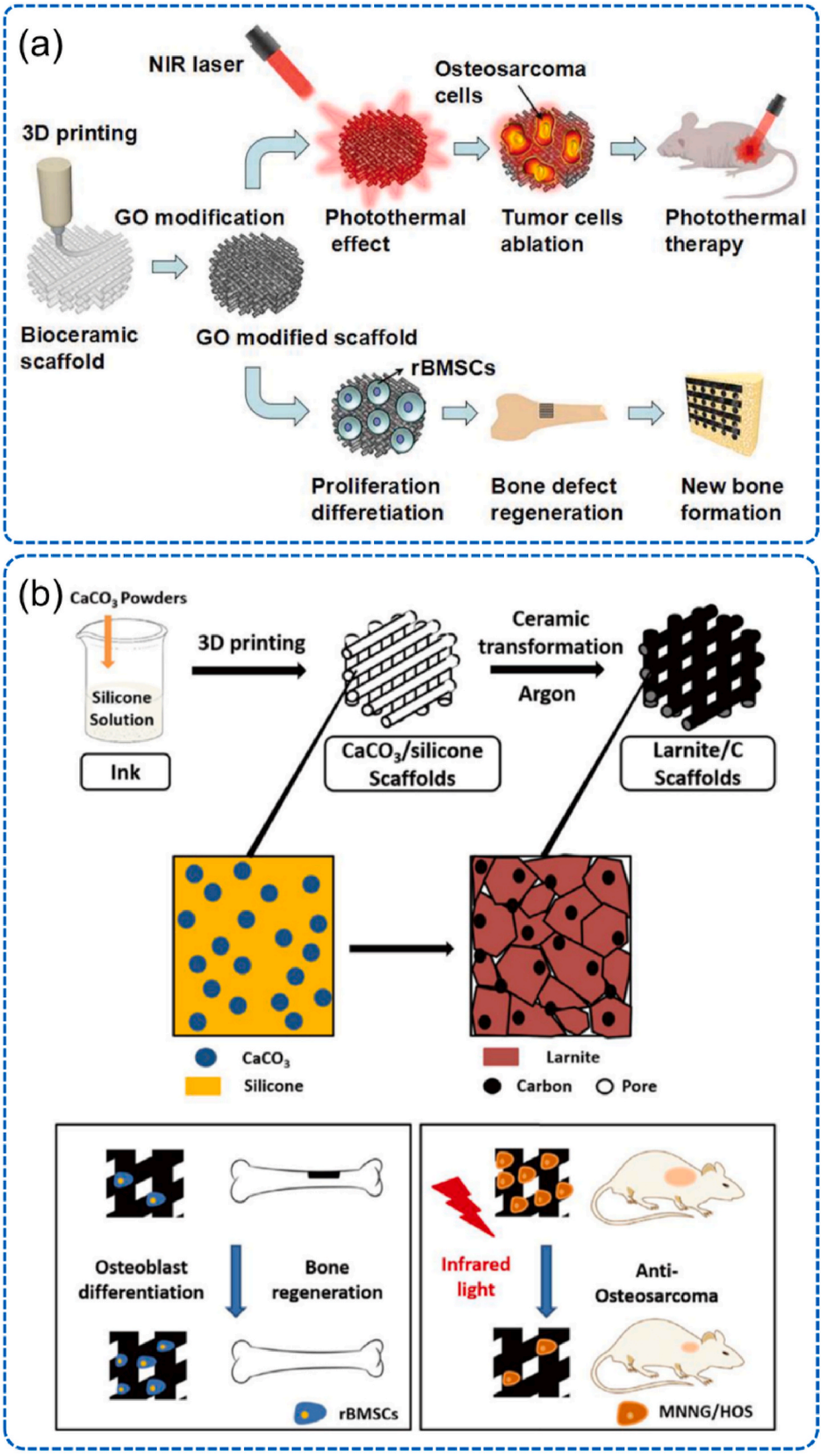

Fig. 6. (a) Preparation of a 3D printing bifuctional GO-TCP scaffold for ablation of tumor cells and promotion of new bone formation. Reproduced with permission from Ref. 55. Copyright 2016 John Wiley and Sons. (b) Fabrication of 3D printing larnite/C scaffolds for PTT and bone regeneration. Reproduced with permission from Ref. 59. Copyright 2020 Elsevier.

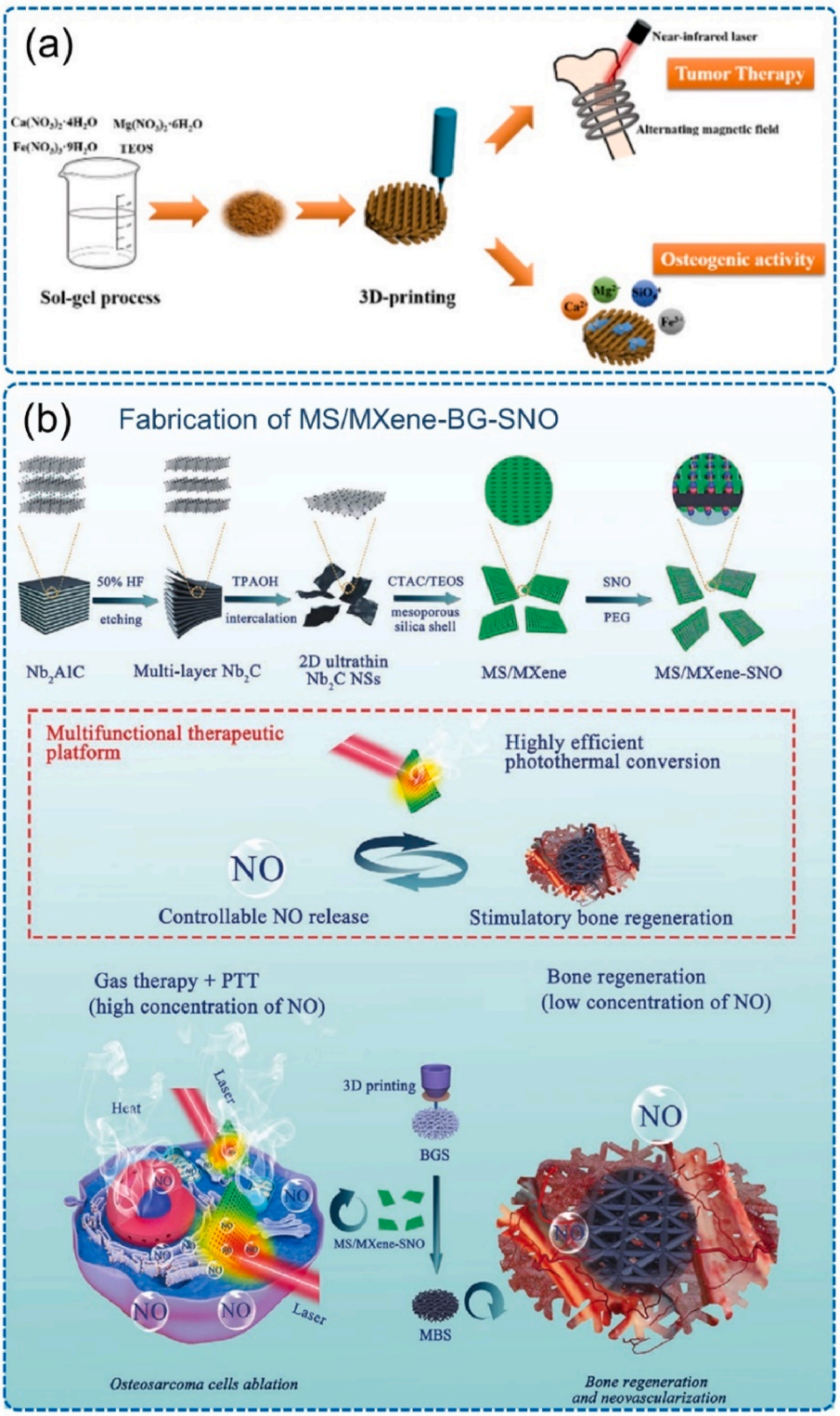

Fig. 7. (a) Preparation of a 3D printing AKT bioceramic scaffold with both tumor-ablation capability *via* the combination of PTT and magnetic therapy and osteogenic bioactivity. Reproduced with permission from Ref. 60. Copyright 2019 American Chemical Society. (b) Fabrication of MS/MXene-BG-SNO scaffolds that are capable to ablate osteosarcoma cells and promote bone regeneration under different NO concentration. Reproduced with permission from Ref. 61. Copyright 2020 John Wiley and Sons.

inducing the phase transition of the phospholipid bilayer or the thermal denaturation of the whole glycoprotein to promote the entrance of delivered molecules into target cells [107,108].

During the recent decade, several photothermal scaffolds/surfaces have been developed as photothermal-poration platforms for effective delivery of various molecules to diverse types of cells, which will be introduced in this section as divided into two categories: (i) photothermal scaffolds/surfaces embedded or deposited with PTAs randomly, and (ii) photothermal surfaces with regular structure (Table 2)

3.1. Photothermal scaffolds/surfaces embedded or deposited with PTAs randomly

Under NIR irradiation, photothermal scaffolds/surfaces embedded or deposited PTAs randomly can produce heat to improve the membrane permeability of the cells cultured on the surfaces, thereby promoting the

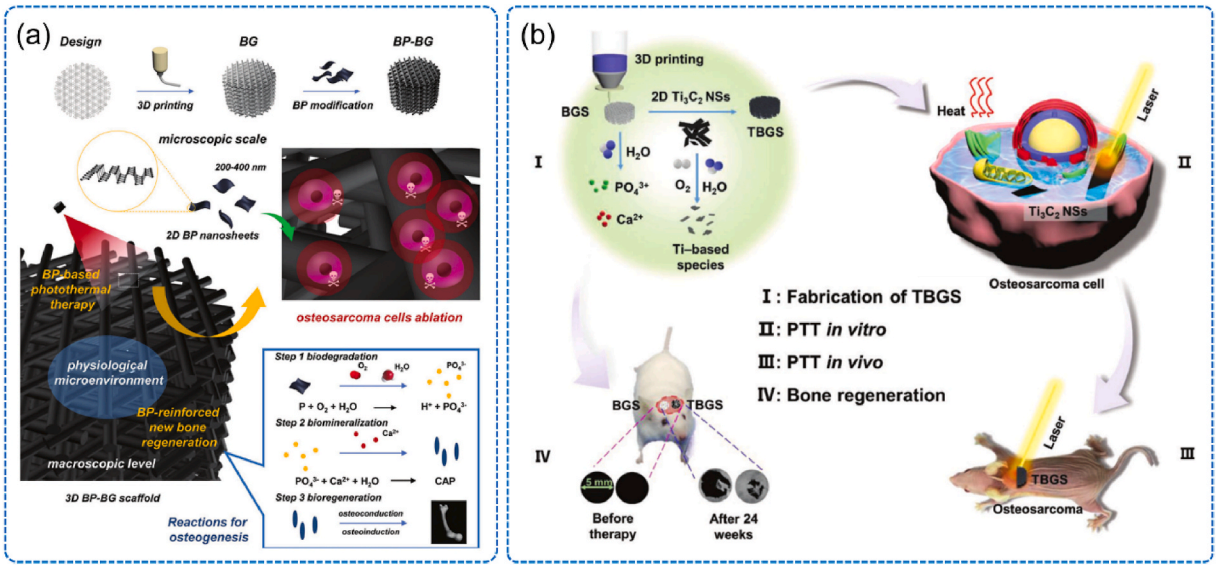

Fig. 8. (a) Preparation of BP-BG scaffolds by integration of 2D BP nanosheets into 3D printing BG scaffolds for elimination of osteosarcoma as well as biomineralization and osteogenesis. Reproduced with permission from Ref. 62. Copyright 2018 John Wiley and Sons. (b) Fabrication process of BG scaffold embedded with Ti_3C_2 nanosheets (TBGS) with biofunction of bone cancer ablation and bone tissue regeneration. I) Fabrication of TBGS and degradation of Ti_3C_2 nanosheets from TBGS; TBGS used for osteosarcoma cell ablation both II) in vitro and III) in vivo; IV) Bone tissue regeneration after implantation of blank BG scaffold and TBGS. Reproduced with permission from Ref. 63. Copyright 2020 John Wiley and Sons.

entrance of exogenous molecules into cells. So far, the PTAs used mainly included gold nanomaterials, PDA nanoparticles, and magnetic nanoparticles [110–113]. Gold-based nanomaterials (such as GNRs and GNPs) have various characters including excellent photothermal effects, good biocompatibility, easily deposition on substrates [126], therefore, a series of surfaces deposited with gold nanomaterials were developed for intracellular delivery *via* photothermal-portation [109–111]. In 2010, Chiou and co-workers developed a cell culture dish immobilized with GNPs by particle bombardment [109]. Under laser irradiation, the modified dish surface generated heat energy to produce water vapor nanobubbles, thus generating the "transient holes" on cell membrane, facilitating the intracellular delivery of molecules. Furthermore, with the assistance of the specific coverage of a photomask, a patterned delivery of fluorescent molecules to human embryonic kidney cells (HEK293) was achieved. However, this method relied on expensive equipment to fabricate the photothermal surface, and it was difficult to prepare a large-area photothermal surface by particle bombardment.

In attempts to solve these problems, Chen and co-workers used a chemical plating method to deposit a layer of dense GNPs (named as GNPL) on the substrate. Compared to the particle bombardment method above-mentioned, the chemical plating method for fabrication of GNPL is simpler, more environment-friendly, more scalable and does not require expensive equipment [127]. Additionally, a large-area surface can be obtained by the chemical plating method. More importantly, compared with scattered GNPs in solution, GNPL composited with dense GNPs has a more excellent photothermal effect [128]. Taking advantages of the characteristics of GNPL, we established a universal platform for delivering various molecules into different cell types with high efficiency [110]. The proposed delivery mechanism was illustrated in Fig. 9a, under NIR irradiation, the moderate heat generated by GNPL resulted in the formation of "transient holes" on cell membrane, thus the exogenous molecules could be entered into cell interior through the "transient holes". The mechanism was confirmed by the results of confocal microscopy, which indicated that the tetra-methylrhodamine isothiocyanate (TRITC)-labeled dextran was delivered into the cell interior, not merely adhered to the outer membrane (Fig. 9b). Although using GNPL outperformed the widely used transfection reagent, Lipofectamine 2000 in gene transfection (i. e. intracellular delivery of plasmid DNA (pDNA)) for c recalcitrant primary cell lines, the efficiency is still not as good as that for easy-to-transfect cell lines. The low efficiency might be resulted from the possible enzymolysis of unprotected pDNA in the extracellular space. In order to enhance the transfection efficiency for hard-to-transfect cells, we further collaborated GNPL with a cationic polymer carrier (polyethylenimine, PEI, 2 kDa) to protect pDNA, realizing high delivery efficiency of plasmid DNA-encoding green fluorescence protein (pGFP) to hard-to-transfect cells (94.0 ± 6.3% for HUVECs, and 88.5 ± 9.2% for mouse embryonic fibroblasts (mEFs)) with high cell viability [111]. Moreover, as a proof-of-concept, a functional pDNA encoding ZNF580 gene (pZNF580) was transfected to HUVECs utilizing this platform, and the "engineered" HUVECs showed enhanced cell attachment in early stage and cell proliferation for long-term culture, showing potentials for endothelialization of blood contacting devices.

Besides gold-based nanomaterials, PDA also has excellent light-to-heat conversion property. Moreover, PDA has been widely used for surface functionalization due to its strong adhesive property regardless of the properties of substrates [129,130]. Therefore, PDA was explored as a photothermal layer for intracellular delivery. For example, Ji, Ren, and co-workers developed a microporous spongy film modified with PDA for gene transfection [112]. In detail, a poly(D, L-lactide-co-glycolide) (PLGA) spongy film with microporous structure was prepared by ultrasonic spray onto polymethyl methacrylate substrate, followed by being coated with PDA and modified by hyaluronic acid with negatively charge for loading pGFP encapsulated with branched PEI (bPEI) (pGFP/bPEI) (Fig. 10a). Under NIR irradiation, the loaded pGFP/bPEI was delivered to the HUVECs attached on the film with high transfection efficiency (85%). Moreover, the spatial control of delivery was realized by controlling the laser irradiation, providing this platform potentials in precision gene therapy. In the following work, they designed another photothermal platform by simply co-depositing PDA and PEI onto the cell culture plate wells, which was easier to prepare and did not need complicated equipment compared to the former PLGA-based photothermal film [113]. Moreover, the PEI pre-immobilized onto surface could increase the loading of pGFP/bPEI complex The produced heat not only promoted the pDNA release form the surface, but also increased the membrane permeability of cells. The probable delivery mechanism was studied by using Sytox (a red dye that is membrane-impermeable) staining assay. As shown in Fig. 10b, no

Table 2
Summary of photothermal scaffolds/surfaces for intracellular delivery of exogenous molecules.[b]

PTAs	Laser wavelength	Strategy of loading PTAs onto surfaces	Delivered molecules	Cell types	Delivery efficiency	Cell viability	Ref
Photothermal scaffolds/surfaces embedded or deposited with PTAs randomly							
GNSPs	532 nm	Bombardment technique	Fluorescent dye	HEK293T cells	N.A.	N. A.	[109]
GNPs	808 nm	Chemical plating method	TRITC-dextran/pGFP	HeLa cells/ mEFs/ HUVECs/ mESCs	HeLa cells with 100%; pGFP delivery to mEFs, HUVECs with 53% and 44%	Near 100%	[110]
GNPs	808 nm	Chemical plating method	pGFP	mEFs/HUVECs	mEFs with 88.5% and HUVECs with 94.0%	80%	[111]
PDA	808 nm	Self-polymerization	pDNA	HUVECs	85%	N. A.	[112]
PDA	808 nm	Self-polymerization	pDNA	HUVECs/293T cells	N.A.	N. A.	[113]
P-MNPs	808 nm	Adsorption via magnetic field	Dextran/pDNA	HeLa/mEFs	67% for pGFP to HeLa; 30% for pGFP to mEFs	>92.6%	[114]
PDA	808 nm	Self-polymerization	Dextran/BSA/pGFP/ZNF580 gene	HeLa/mEFs/ HUVECs/mDCs	>99%	60% for mDCs 90% for other cells	[115]
GNRs	785 nm	Microcontact printing	DOX	A498 cells	N. A.	N. A.	[116]
GNRs	808 nm	Embedding GNRs into fibers during electrospinning process	pFGF	NIH3T3	>90%	>90%	[117]
Photothermal surfaces with regular structure							
TPS Au surface	800 nm/ 1064 nm	Nanofabrication	FITC-dextran/Calcein	HeLa cells	95% for the smallest molecules	Up to 98%	[118,119]
TPS TiN MPAs	1064 nm	Anisotropic etching	Calcein dye	HeLa cells	N. A.	>90%	[120]
metallic (Ti) tips	532 nm	Sputter deposition	Calcein (0.6 kDa)/FITC-dextran (2000 kDa) /bacterial enzyme β-lactamase (29 kDa)/pGFP	Ramos suspension B cells	84%, 45% and 58% for calcein, FITC-dextran and pGFP delivery	>89%	[121]
GNDAs	532 nm	Chemical lift-off lithography	Calcein (0.6 kDa)	HeLa cells	>98%	>98%	[122]
GNTs			PI	NIH3T3	N. A.	N. A.	[123]
Ti thin films	1064 nm	Focused ion beam milling and secondary electron lithography	FITC-dextran/polystyrene beads/ enzyme/bacteria	HeLa/NHDFs/ PB-MDMs/ RPTECs	N. A.	>90%	[124]
SiNWAs	808 nm	Chemical etching method	RBITC-BSA/pGFP	HeLa/Ramos/T cells	100%, 83% and 80% for pGFP transfection to HeLa, Ramos and T cells, respectively	>95%	[125]

[b] Abbreviations: gold nanosphere particles (GNSPs); gold nanotubes (GNTs); gold nanodisk arrays (GNDAs); porous magnetic iron oxide nanoparticles (P-MNPs); gold-coated thermoplasmonic substrates (TPS-Au); TiN-coated thermoplasmonic substrates (TPS-TiN); silicon nanowire arrays (SiNWAs); Tetramethylrhodamine isothiocyanate/fluorescein isothiocyanate-labeled dextran (TRITC/FITC-dextran); plasmid DNA-encoding green fluorescence protein (pGFP); pDNA encoding fibroblast growth factor/ZNF580 gene (pFGF/pZNF580); doxorubicin (DOX); rhodamine B isothiocyanate-labeled bovine serum albumin (RBITC-BSA); mouse embryonic fibroblasts (mEFs); human umbilical vein endothelial cells (HUVECs); mouse dendritic cells (mDCs); peripheral blood monocyte-derived macrophages (PB-MDMs); renal proximal tubule epithelial cells (RPTECs).

obvious fluorescence was observed for the cells without NIR irradiation, suggesting their intact membranes. In contrast, red fluorescence was observed for the cells after NIR irradiation, and more fluorescent cells after longer irradiation time. In addition, NIR irradiation also led to the release of lactate dehydrogenase (LDH, a cytosolic enzyme) from cells. These results together indicated that the heat generated by the PDA layer disturbed the cell membrane, forming transient pores and thus facilitating the transportation and exchange of molecules inside and outside the cells.

In addition to high-efficiency delivery of functional molecules, harvesting the "engineered" cells effectively and non-traumatically from the surfaces is also important for the further fundamental research or clinical utilizations such as *ex vivo* cell-based therapies, e.g., hematopoietic stem cells transplantation to reconstitute dysfunctional cell lineages [131] and T-cell immunotherapy [100], in which the "engineered" cells should be injected to patients. In this regard, we developed a nanoplatform based on porous magnetic iron oxide nanoparticles (P-MNPs) with photothermal properties for macromolecular delivery [114]. Before cell seeding, a layer of P-MNPs was deposited on the bottom of the culture plate used a magnetic field, enabling more efficient heat transfer between the cells and P-MNPs, compared with suspended P-MNPs in solution. Under NIR irradiation, successful delivery of pGFP to cells were obtained with negligible cytotoxicity. Most importantly, 97% of the "engineered" cells could be harvested simply by treatment of proteolytic enzymes (e.g. trypsin) while high viability for subculture was maintained, which is crucial for further practical application of the delivery system. Although the "engineered" cells could be recovered from surface of P-MNPs layer by trypsin treatment, the delivery efficiency of pGFP to cells using p-MNPs layers was not very high, especially for the hard-to-transfect cell lines, while trypsin treatment may impair the cell viability. To circumstance this problem, we developed a two-in-one platform for high-efficiency intracellular delivery and cell harvest by grating thermo-responsive PNIPAAm chains from a PDA layer to achieve a PDA/PNIPAAm hybrid film [115]. Because of the excellent photothermal property of PDA, this hybrid film delivered diverse molecules to multiple cell types including hard-to-transfect cells (e.g. HUVECs, mEFs and mouse dendritic cells (mDCs)) under proper NIR irradiation. Moreover, due to the thermo-responsive property of

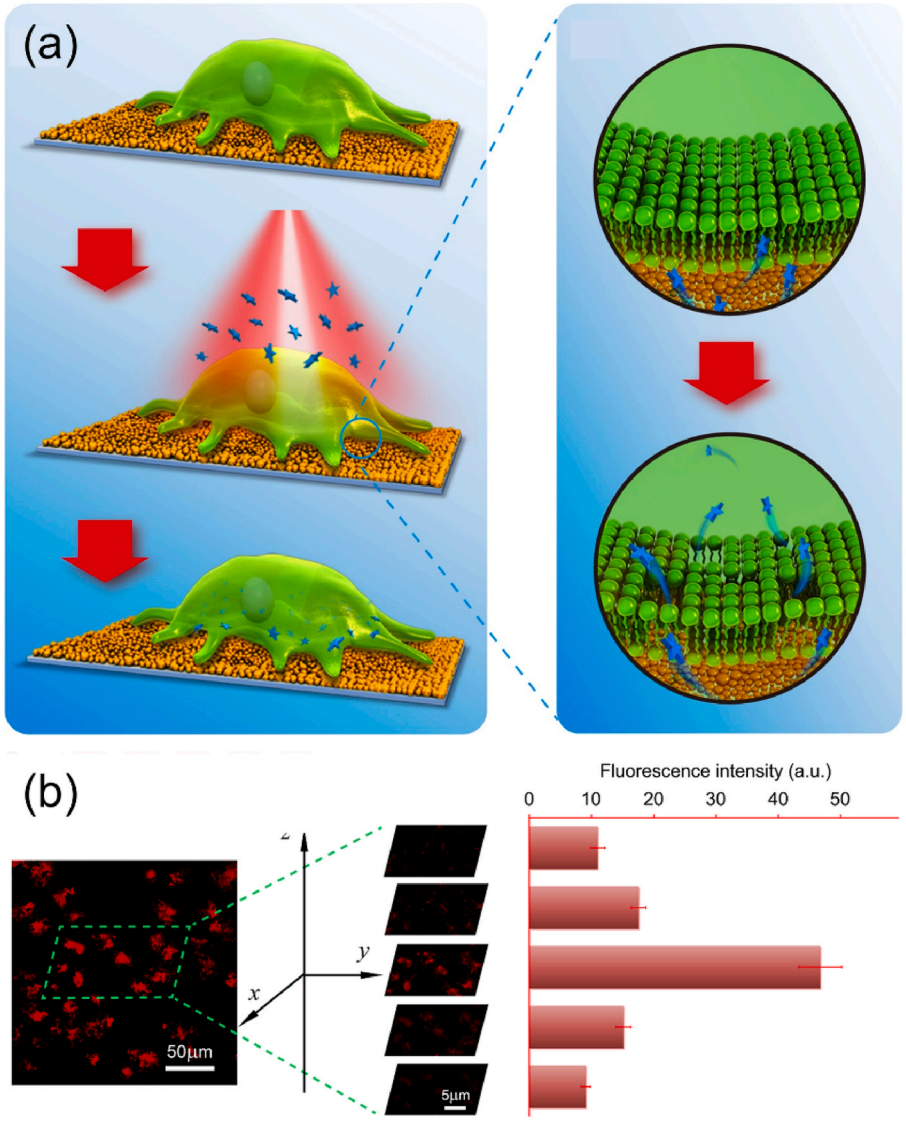

Fig. 9. (a) Proposed mechanism of delivery of exogenous molecules into living cells cultured on a GNPL under NIR irradiation. (b) Representative confocal microscopy images of HeLa cells delivered with TRITC-dextran using a Z-stack scan mode. Reproduced with permission from Ref. 110. Copyright 2016 John Wiley and Sons.

PNIPAAm, the cells with delivered molecules were released from the film simply by lowering the temperature of cell medium (Fig. 11a), because the surface of PDA/PNIPAAm hybrid film became more hydrophilic state from hydrophobic state [132]. More importantly, the released cells preserved good viability for further subculture, and the delivered biomolecules realized their specific functions. For example, using this platform, recalcitrant HUVECs were transfected with ZNF580 gene, showing improved migration ability compared with untransfected cells (Fig. 11b).

3.2. Photothermal surfaces with regular structure

Although the above-mentioned photothermal scaffolds/surfaces are relatively easy to prepare, they still have some shortcomings. For example, it is difficult to well control the uniformity of the distribution of PTAs on the surface, which may lead to uneven heating of the cells attached to the surface under NIR irradiation, resulting in inconsistent delivery. In addition, a small part of immobilized PTAs or their fragments may be detached from the surface and delivered into cell interior, causing potential cell cytotoxicity [110,133]. To this end, a series of array-type surfaces with photothermal effects were developed including nanopyramid arrays (Scheme 2a), nanodisk arrays (Scheme 2b), nanowire arrays (Scheme 2c) and hollow nanohole arrays (Scheme 2d) to deliver exogenous molecules to the cells [119,122,124,125].

Most of the array-type photothermal surfaces were fabricated by printing or etching to give a uniform surface topography. For example, Mazur, Wolf and co-workers developed plasmonic tipless pyramid arrays using lithographic printing [118]. Under NIR irradiation, the heat produced by the plasmonic arrays resulted in the generation of vapor nanobubbles and pressure waves, improving the membrane permeability of attached cells and promoting the calcein delivery with efficiency of 80%. However, scaling up these arrays using e-beam lithography is relatively difficult and the tipless pyramids need angular gold deposition by a thermal evaporator with rotating stage, affecting precision in reproducibility for large-area samples. To this end, they further developed relatively large gold-coated thermoplasmonic arrays (14 × 14 mm) fabricated by photolithography and template-stripped methods [119]. These arrays presented an upright pyramid array structure and had excellent photothermal effect (Fig. 12a). Under nanosecond laser irradiation, fluorescence-labeled dextrans with different molecular weight were delivered into HeLa cells successfully, in particular, for 150 kDa dextran, delivery efficiency of 73.9% and cell

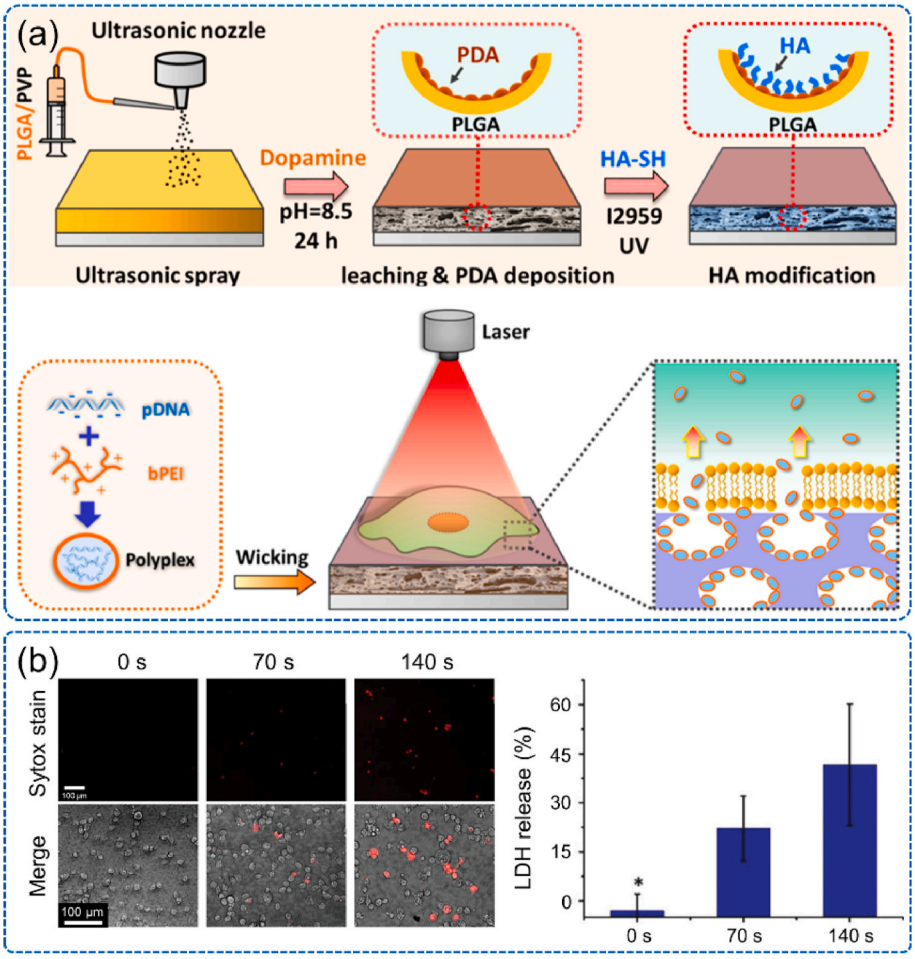

Fig. 10. (a) Top: Preparation of a PLGA spongy film sequentially modified with PDA and HA. Down: Loading of pDNA/bPEI complexes in modified PLGA spongy film for further intracellular delivery under NIR irradiation. Reproduced with permission from Ref. 112. Copyright 2019 American Chemical Society. (b) Typical fluorescence images of cells delivered with Sytox on PDA-PEI photothermal matrix under different NIR irradiation time (left). Release of LDH from the cells under same condition is also shown (right). Reproduced with permission from Ref. 113. Copyright 2019 The Royal Society of Chemistry.

viability of 98% were achieved. More importantly, using this platform, high throughput of 50,000 cells/min was offered, and the throughput could be scaled up as necessary. It is noted that the mechanical property of gold is a weak and thus the gold film falls off the substrate easily, which may cause residual cell toxicity for long-term clinical applications [134]. In order to overcome this problem, Mazur and co-workers used robust titanium nitride (TiN) instead of gold to coat thermoplasmonic arrays for intracellular delivery, avoiding the potential risks of gold materials in clinic applications. Under 1064 nm NIR irradiation, calcein was delivered to HeLa cells [120]. It is found that template stripping process was relatively complex for sample preparation. To this end, they constructed a gold nanodisk arrays (GNDAs) with large area by a soft lithography and chemical lift-off lithography in a simple and cost-effective way [122]. Here, the substrate (e.g. Si wafer) was coated with gold film functionalized with a self-assembly monolayer (SAM) of hydroxyl-terminated alkanethiol (11-mercapto-1-undecanol). Then a patterned PDMS stamp activated by oxygen plasma was pressed onto the surface and then lifted to selectively remove the contacted SAM. Similarly, the PDMS stamp was rotated 90° and was pressed onto surface again, generating 2D nanosquare SAM region. Finally, GNDAs could be fabricated after removing the exposed metal *via* wet etching (Fig. 12b). Under nanosecond laser irradiation, delivery of calcein green with high efficiency (>98%) was achieved and the cell viability was well maintained (>98%).

Successful delivery of functional molecules into suspension cells, in particular immune cells, plays an crucial role in immunotherapy such as cancer vaccines and CAR-T therapy [135]. However, different with adherent cells that attach on substrate surfaces naturally, suspension cells typically have insubstantial duration of cell-surface contact, making it more difficult to efficiently deliver exogenous molecules to suspension cells using currently available photothermal surfaces as mentioned above. Aiming at this problem, Chiou and co-workers constructed a uniform microwell array with a 3D nanoscale titanium-coated tips through self-aligned micromachining [121]. Due to the action of gravity, the suspension cells could self-position the microwells and neared sharp tip structures (Fig. 13a). Under NIR irradiation, diverse molecules with different sizes including calcein green, FITC-dextran and pGFP were efficiently delivered into suspended Ramos cells located in microwells with a high throughput of >100,000 cells per minute. In addition, they chose β-lactamase (a bacterial enzyme) as the model exogenous cargo to investigate the biological activity of delivered cargo after entry into cell interior. After the delivery of β-lactamase to cells, the emission wavelength of CCF4 converted from the CCF4-AM as a substrate was changed from 520 nm to 447 nm (Fig. 13b), exhibiting high biological activity.

Although these solid arrays mentioned above show good performance for intracellular delivery, some limitations still exist. One is that the delivered molecules dispersed into cell medium or loaded on substrate surfaces gradually taper off with the extension of delivery process. Another is that it is tedious and difficult to co-deliver or sequential deliver different molecules into the same cell repeatedly. Alternatively, hollow nanohole arrays that are composed of a dense array of hollow nanoholes are promising to solve these problems. The bottom of nanohole arrays can be connected to a microchannel or a fluid storage device where the delivered molecules are stored in, facilitating the delivery of the same or different molecules continuously and repeatedly to the cells attached on the upper surface of the nanohole arrays [123,124]. For example, Chiou and co-workers developed a massively parallel

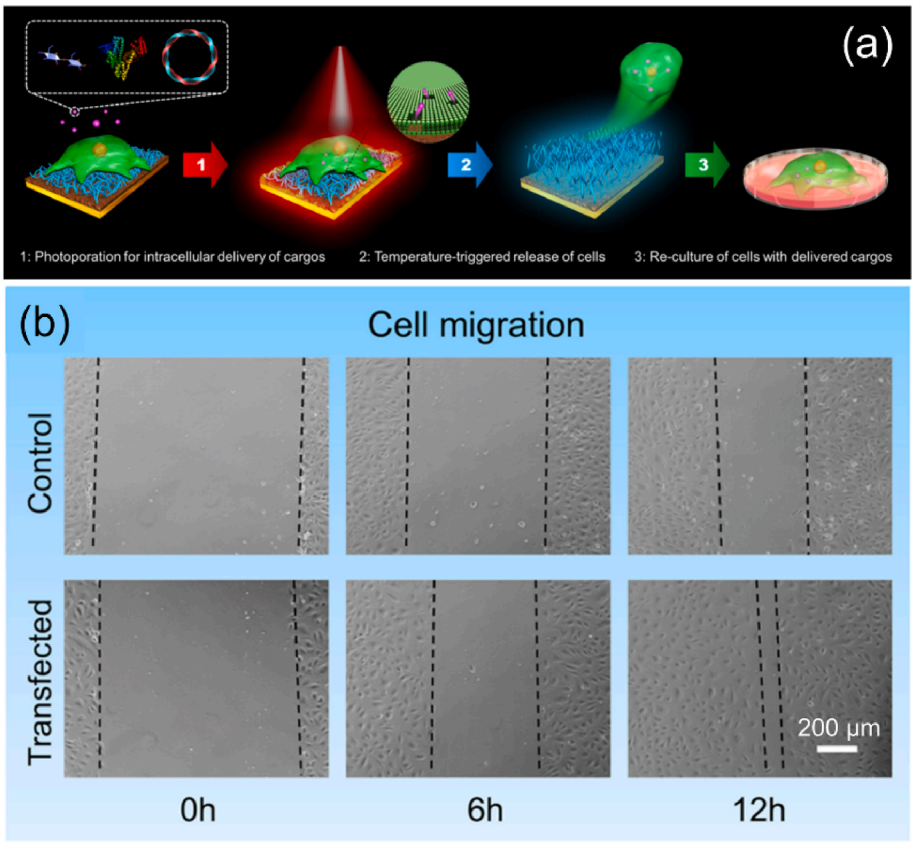

Fig. 11. (a) Scheme of the performance of intracellular delivery under NIR irradiation and cell harvesting by low-temperature treatment of PDA/PNIPAAm hybrid film. (b) Typical optical microscopic images showing the migration of HUVECs transfected with ZNF580 gene at different times. Reproduced with permission from Ref. 115. Copyright 2019 American Chemical Society.

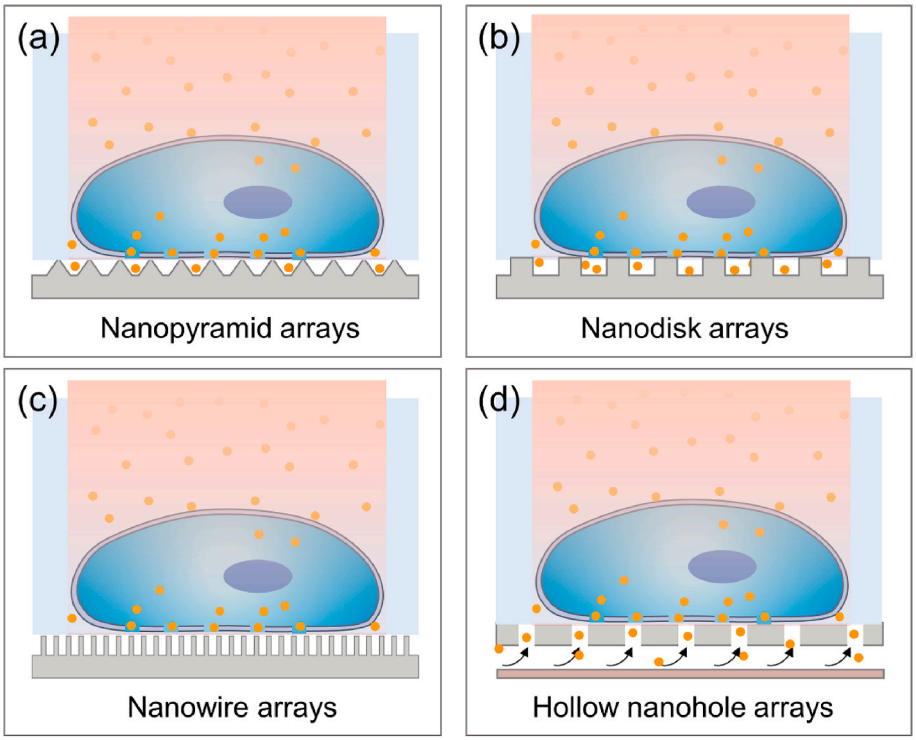

Scheme 2. Different surface-mediated photothermal-poration methods based on diverse nanoarrays with different structures. (a) Nanopyramid arrays, (b) Nanodisk arrays, (c) Nanowire arrays, and (d) Hollow nanohole arrays.

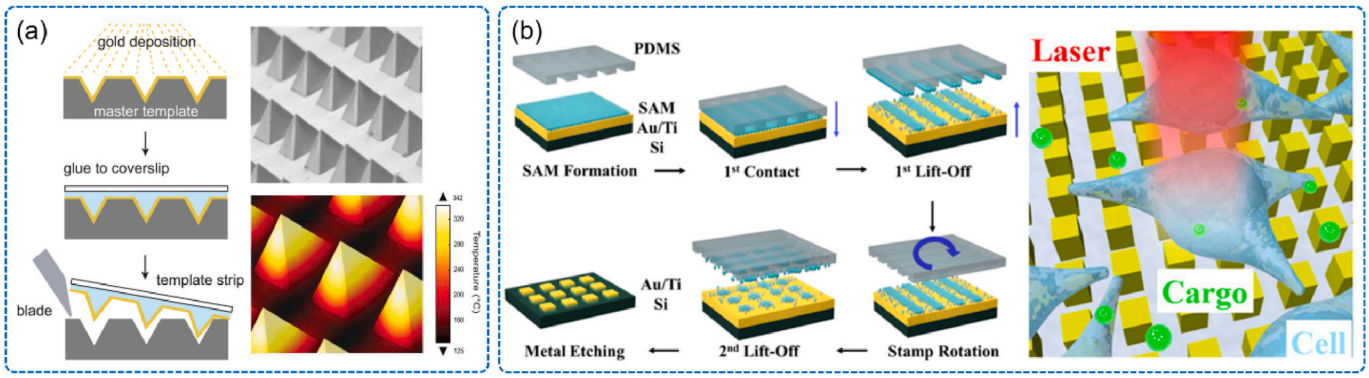

Fig. 12. (a) Left: fabrication of gold-coated thermoplasmonic nanopyramid arrays using photolithography and template-stripped methods. Right: a typical SEM image and temperature change of the resulted nanopyramid arrays under NIR irradiation. Reproduced with permission from Ref. 119. Copyright 2017 American Chemical Society. (b) Left: fabrication process of GNDAs using double-patterning chemical lift-off lithography. Right: schematic illustration of delivery of cargoes into living cells cultured on GNDAs under NIR irradiation. Reproduced with permission from Ref. 122. Copyright 2020 American Chemical Society.

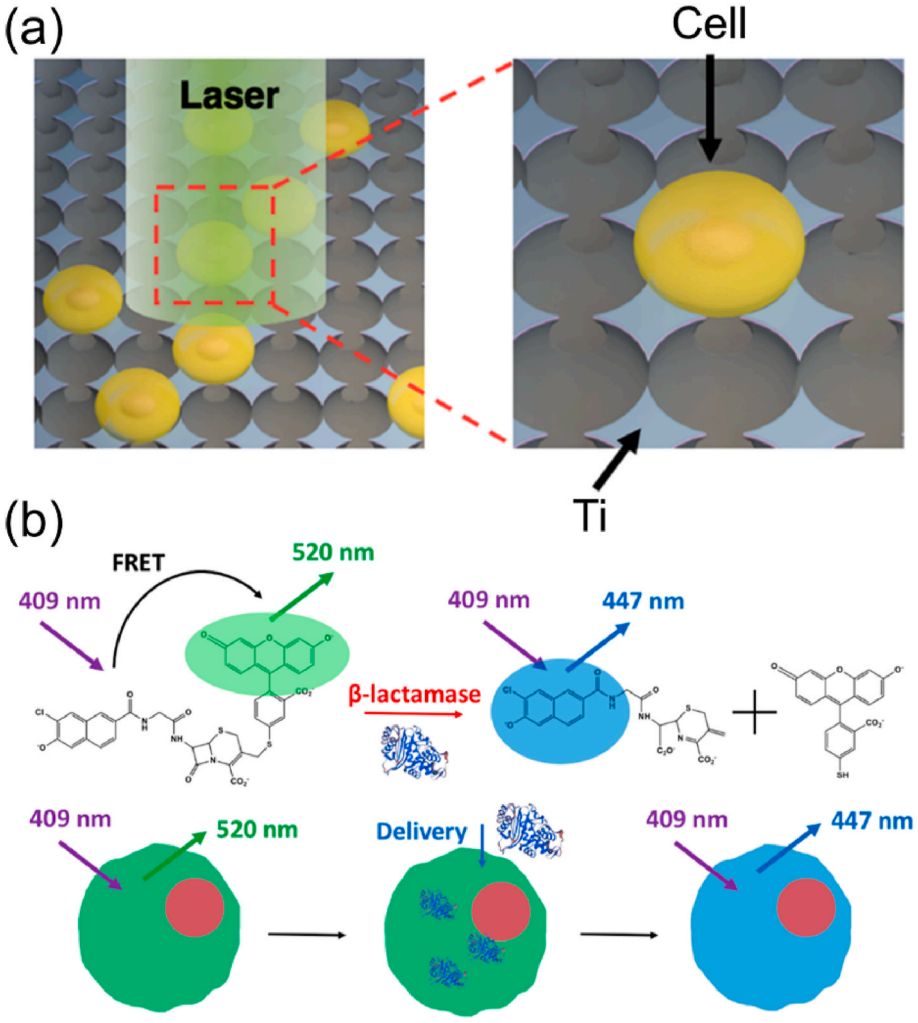

Fig. 13. (a) Schematic illustration of delivering molecules into suspension cells self-positioned within microwells under NIR irradiation. (b) Mechanism of CCF4-AM substrate functionality in characterization of β-lactamase. Reproduced with permission from Ref. 121. Copyright 2019 American Chemical Society.

photothermal biophotonic laser-assisted surgery tool (BLAST) for delivery of diverse cargoes with sizes in micrometer-scale [124]. This BLAST platform consists of an array of hollow *trans*-film nanohole coated with titanium film on the side walls of these holes. Underneath the hollow nanohole arrays was an array of short and vertical silicon channels that provide fluid passage for cargo delivery and microfluidic storage used to store delivered molecules (Fig. 14a). Under laser irradiation, due to the photothermal property of metallic titanium thin films, the cavitation bubbles caused by heat and vaporization of adjacent water layers grew, aggregated and collapsed, resulting in strong fluid flow, disrupting the cell membrane and facilitating the cargoes stored in the bottom device entering the cells (Fig. 14b). Using this platform,

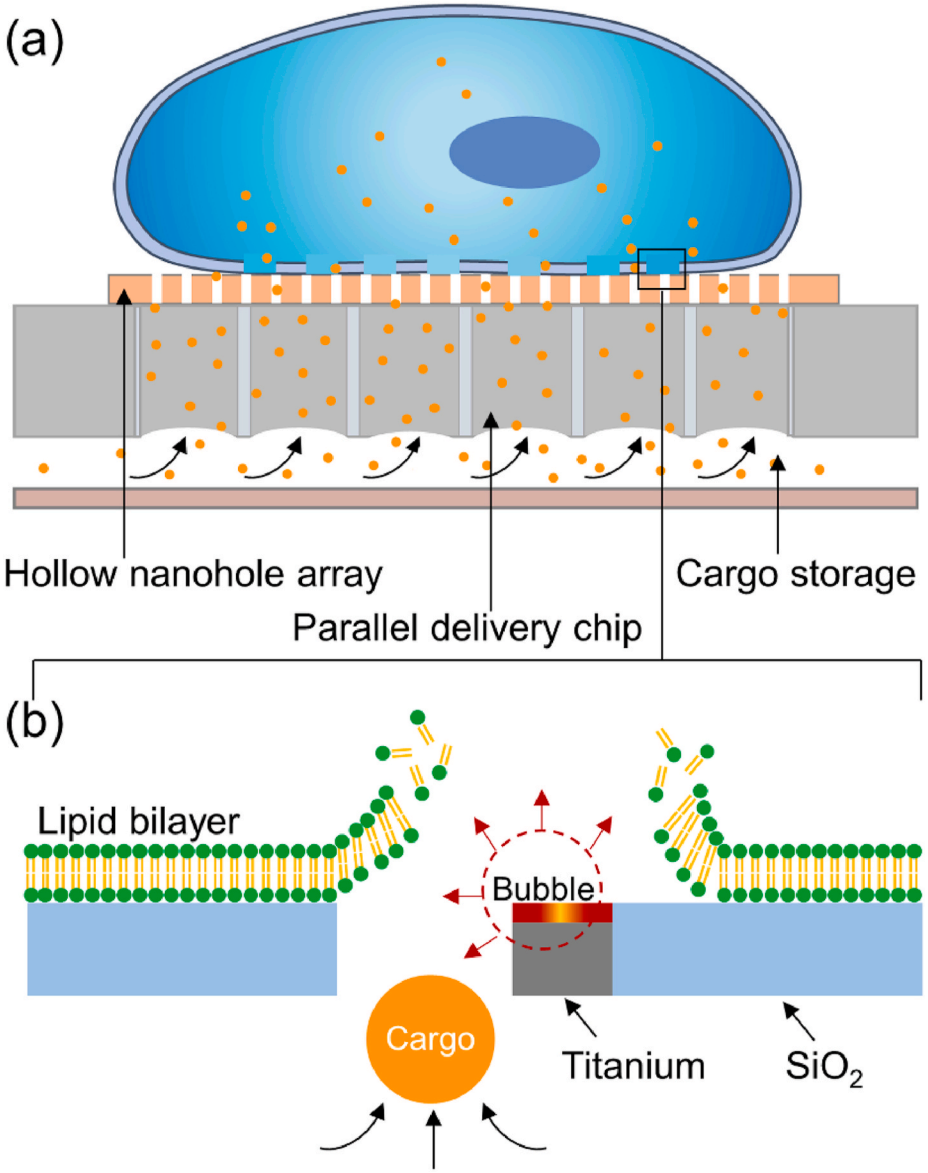

Fig. 14. Schematic illustration of (a) the BLAST large-cargo delivery platform and (b) the delivery of cargoes into living cells cultured on the hollow nanohole arrays under NIR irradiation.

various cargoes including antibodies, enzymes, nanoparticles, and living bacteria were efficiently delivered into multiple cell types involving easy-to-transfect cells and hard-to-transfect cells with high throughput, high delivery efficiency, and low cytotoxicity. Importantly, this platform may sequentially deliver multiple exogenous molecules into the same cell through the bottom channel, and thus has potential applications in cell reprogramming [124].

Non-destructive harvesting of "engineered" cells is important for regenerative medicine and *ex vivo* cell-based therapy [101]. Although such cell harvest was achieved by using a temperature-responsive photothermal surface as mentioned in Section 3.1 [136], however, low temperature treatment may impair cell viability and function and is not suitable for some sensitive cell types. In this regard, we developed a facile platform by combination of silicon nanowire arrays (SiNWAs) and sugar-responsive polymers containing phenyl boronic acid (PHB) that can recognize cells over-expressed sialic acid [125]. As illustrated in Fig. 15, SiNWAs-PHB could capture HeLa cells, Ramos cells and T cells with high efficiency due to the 3D topography structure of SiNWAs and specific recognition of PHB [137,138], and realize efficient molecular delivery to the captured cells under NIR irradiation due to the excellent photothermal properties of SiNWAs. It is noted that the transfection efficiency of pGFP into recalcitrant suspension T cells was as high as 80%, which was significantly higher than that by using other reported approaches or commercially available transfection agents. Moreover, the "engineered" cells could be recovered non-traumatically from the surface by nontoxic fructose treatment due to the sugar-responsive characteristic of the boronate ester bonds between PHB and cell membrane over-expressed sialic acid. The harvested cells preserved viability and proliferation ability for further use.

4. Photothermal surfaces for cell detachment and cell sheet harvest

Dynamic modulation of cell adhesion-detachment on functional surfaces is of importance in cell biology and tissue engineering and plays a critical role in diverse biomedical applications including isolation of circulating tumor cells (CTCs) from blood for clinical diagnostics [139,140], and harvest of viable and intact cell sheets for transplantation [3,141]. Stimuli-responsive biointerfaces with dynamic property and programmable features exhibit unprecedented ability to modulate

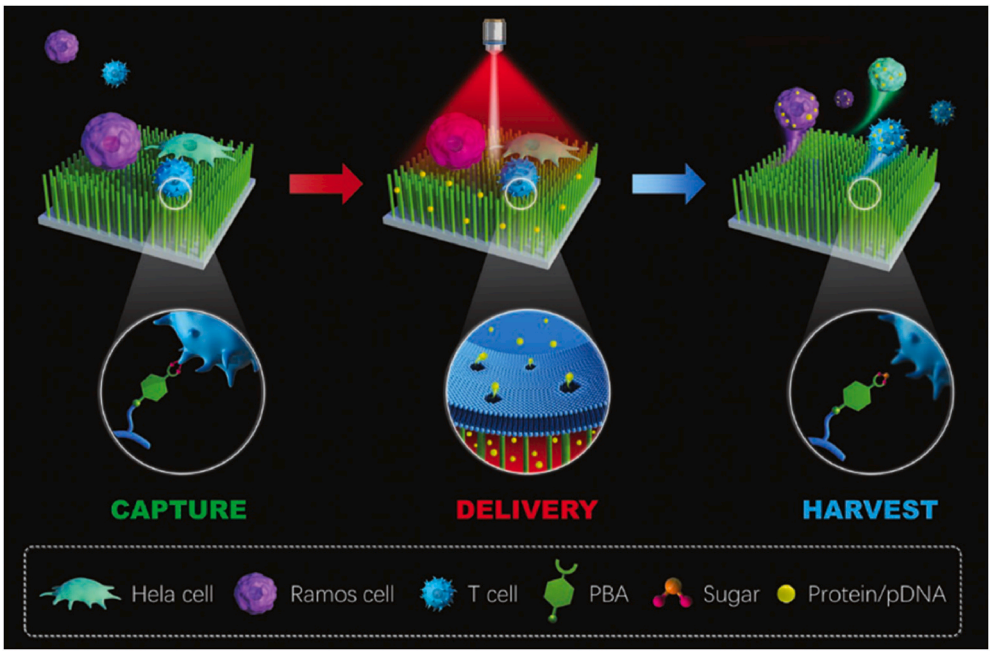

Fig. 15. Scheme of a "all-in-one" platform integrating cell capture, intracellular delivery and engineered cell harvesting. Reproducedd with permission from Ref. 125. Copyright 2020 John Wiley and Sons.

cell-surface interactions. In particular, thermo-responsive surfaces based on PNIPAAm have been well investigated to achieve capture and release of target cells and even whole cell sheets [142,143]. Compared to other stimuli (e.g. pH, electricity, enzyme), thermal stimuli for dynamic modulation of cell adhesion-detachment is easier to operate and more biocompatible. However, it is still challenging to realize precise control of regulating cell detachment for these conventional thermo-responsive surfaces. Alternatively, photothermal surfaces change the surface temperature through the produced heat under NIR irradiation, thus achieving the well control of cell detachment in time and spatial compared to the conventional thermo-responsive surfaces, making them good platforms for dynamic modulation of cell adhesion-detachment. The specific modulation mechanisms of these photothermal surfaces rely on the changes of surface properties in response to the surface-generated heat as illustrated in Scheme 3: (i) dissociation of the binding between responsive materials tethered on surfaces or interactions between cells and surfaces (Scheme 3a), (ii) change of properties of thermo-responsive polymers tethered on the surfaces (Scheme 3b), and (iii) dissolution of the "sacrificial layer" coated on the surfaces (Scheme 3c). In this section, we focus on the recent developments of these photothermal surfaces for dynamic modulation of cell adhesion-detachment, which are divided into the two categories including (i) photothermal surfaces for cell detachment and (ii) photothermal surfaces for cell sheet harvest (Table 3).

4.1. Photothermal surfaces for cell detachment

Thermo-responsive DNA that the double strands could dissociate by increasing temperature is a good candidate for fabrication of photothermal surfaces to achieve modulation of cell adhesion-detachment. For example, Qu and co-workers developed a NIR- and pH-dual-controlled surface to catch-and-release cells reversibly [144]. In detail, an indium tin oxide (ITO) surface was modified with PDA-functionalized graphene (PDA-GO) and GNRs as PTAs, sequentially covalently linked with amino-modified duplex DNA (dsDNA, composed by sequences of C-rich DNA1 and G-rich DNA2) through the bonding between the amine group of DNA1 and the catechol group of PDA, and finally arginine-glycine-aspartic acid (RGD) as bioadhesion ligand to promote cell adhesion was coupled on DNA2. Due to the recognition of RGD to cells, the modified photothermal surfaces could capture cells effectively. Under NIR irradiation, the generated heat by PDA-GO and GNRs disassembled the dsDNA, thus the captured cells were non-traumatically detached from the surface. In addition, decrease of pH also led to the dissociation of dsDNA and thus inducing detachment of cells. (Fig. 16a). In another work, Casares, Marzan and co-workers developed a multifunctional and versatile plasmonic substrate for cell growth, controlled detachment and substrate regeneration under remote NIR irradiation [146]. Firstly, the plasmonic substrate was prepared by depositing small GNPs "seeds" for further chemical growth to form anisotropic GNPs. Thiolated cyclic RGD peptides (c-RGD) were then modified on the surface via thiol chemistry for promoting the adhesion of integrin-rich cells. Under NIR irradiation, most cells were detached from surfaces of plasmonic substrate and c-RGD-modified plasmonic substrate without compromising cell viability, while almost no cells adhered on pristine glass were released (Fig. 16b). It is found that the efficiency of cell detachment was related to the average cell area. For example, HUVECs had the largest adhesion area on the surface of the plasmonic substrate and it achieved cell detachment in a short time of 5 min, significantly faster than other cells with a small contact area. The localized photothermal effect was considered to be the primary driving force of cell detachment [148]. As the contact area between cells and surfaces increased, the temperature at the interface of cells and GNPs was getting higher and higher, thereby accelerating the detachment of the cells. Moreover, the photothermal surface after detaching the captured cells could be re-used for another cell adhesion-detachment cycle [146].

Compared with graphene and gold-based nanomaterials, organic photothermal polymers have more easily adjustable photophysical properties and better biocompatibility. Kim and co-workers coated the surface of cell culture dishes with a nanofilm of photothermal poly (3, 4-ethylenedioxythiophene) (PEDOT) using solution casting polymerization (SCP) technology and tuned doping level of PEDOT film *via* electrochemistry for selective collection of mesenchymal stem cells (MSCs) [145]. Under NIR irradiation, the PEDOT film converted absorbed light energy to heat to break down the linkage between the integrin of cells and the ECM proteins, thereby releasing the attached MSCs. The photothermal property of PEDOT film was affected by doping state and

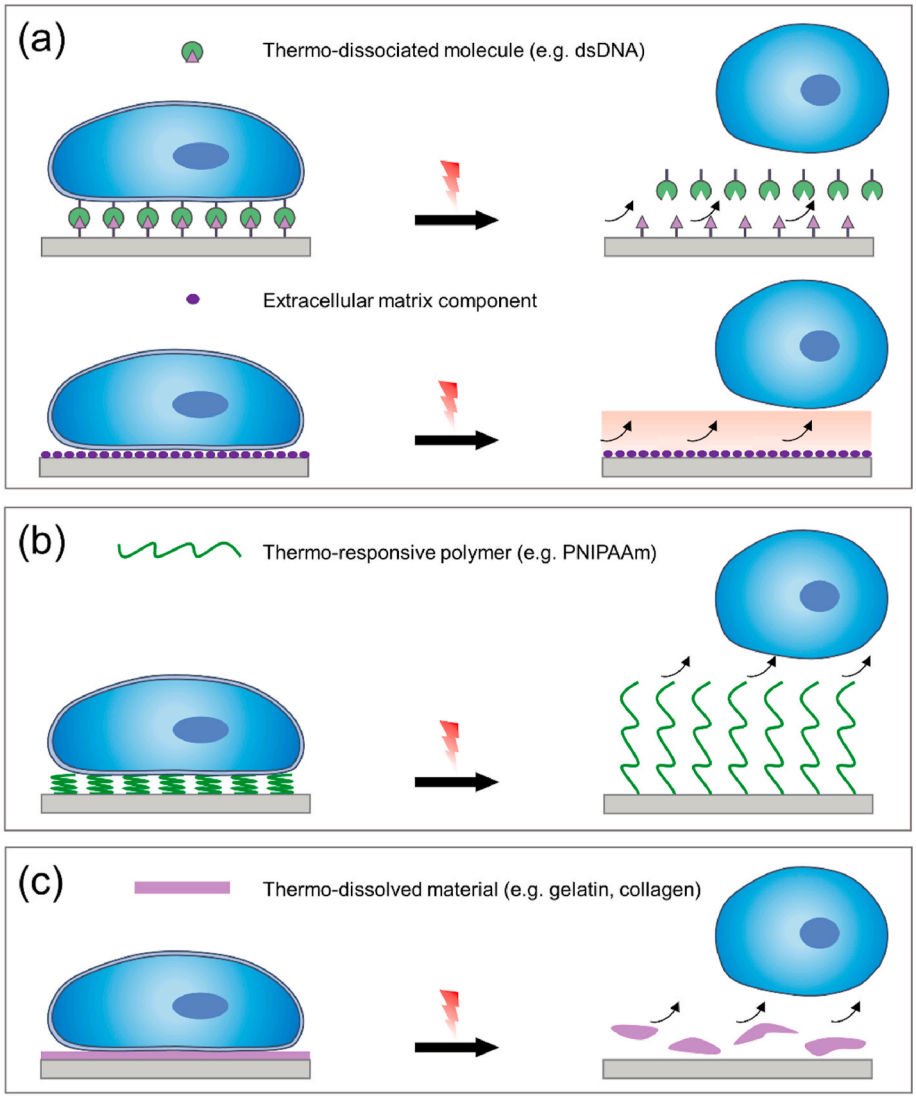

Scheme 3. Schematic illustration of NIR-triggered release of cells from photothermal surfaces by (a) dissociation of the binding between responsive materials tethered on surfaces (Top) or interactions between cells and surfaces (Down), (b) change of the properties of grafted polymer chains (green lines) on the photothermal surfaces and (c) dissolution of the "sacrificial layer" (purple shapes) coated on the photothermal surfaces.

Table 3
Summary of photothermal surfaces for detachment of cells and harvest of cell sheets.[c]

PTAs	Laser wavelength	Responsive materials	Matrix materials	Cell type	Applications	Ref.
rGOs/GNRs	808 nm	NIR/pH-responsive dsDNA	ITO	HUVEC	Capture and release of cells	[144]
PEDOT	808 nm	PEDOT	Cell culture surface	MSC	Selective harvest of cells	[145]
GNPs	980 nm	N. A.	Glass	HeLa cell/A549/HUVEC/J774 cell/ 3T3 fibroblast	Selective detachment of cells	[146]
SiNWAs	808 nm	PNIPAAm	SiNWAs	MCF-7	Capture and release of cancer cells	[147]
GNSTs	785 nm	N. A.	ITO/glass	Glioblastoma cell (U87-GFP)	"Point-and-shoot" selective removal of cells	[148]
GNRs	980 nm	Gelatin	Gelatin	MCF-7	Capture and release of cancer cells	[149]
MoS_2	808 nm	Gelatin	ITO	MCF-7	Capture-in situ detection-release of cancer cells	[150]
PEDOT	808 nm	Collagen	Polystyrene	human fibroblast	Harvest of cell sheets	[151]
PEDOT	808 nm	Collagen	Polystyrene	hADSC	Large-Area and multiple production of cell sheets	[152, 153]
Gradient PEDOT	808 nm	Collagen	Polystyrene	Fibroblast/C6 cell/HeLa cell/3T3 cell	Harvest of cell sheets along a predetermined direction	[154]

[c] Abbreviations: Reduced graphene oxide (rGO); Indium tin oxide (ITO); Gold nanostars (GNSTs); Duplex DNA (dsDNA, composed by sequences of C-rich DNA1 and G-rich DNA2); Mesenchymal stem cell (MSC); Poly(3,4-ethylenedioxythiophene) (PEDOT); harvested human adipose-derived stem cell (hADSC).

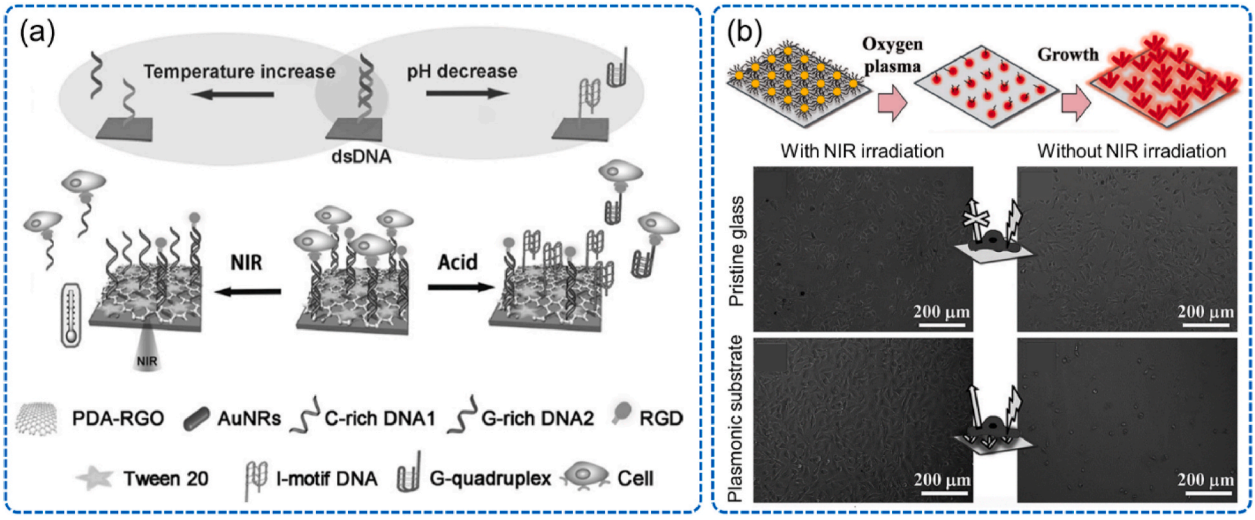

Fig. 16. (a) Scheme of a NIR/pH dual responsive surface based on DNA achieving reversible capture and release of cells. Reproduced with permission from Ref. 144. Copyright 2013 John Wiley and Sons. (b) Top: fabrication of gold nanomaterials-based plasmonic substrates. Down: detachment of HeLa cells from a pristine glass surface and a plasmonic substrate under NIR irradiation. Reproduced with permission from Ref. 146. Copyright 2016 John Wiley and Sons.

thickness of PEDOT film and could be simply modulated by electrochemical method or SCP process. Thicker PEDOT film exhibited better cell release efficiency. Moreover, it was possible to achieve cell detachment in certain area and certain shape by controlling the NIR laser beam correspondingly, showing potential for single cell separation.

In addition to dissociation of the binding between responsive materials tethered on surfaces or interactions between cells and surfaces, there are other approaches such as change of properties of thermo-responsive polymers tethered on the surfaces and dissolution of the "sacrificial layer" coated on the surfaces for cell detachment. As shown in Fig. 17a, Wang and co-workers developed a NIR-responsive surface based on PNIPAAm modified SiNWAs (SiNWAs-PNIPAAm) for controlled capture and release of cancer cells [147]. Under NIR irradiation, the heat produced by SiNWAs made PNIPAAm chains collapsed and hydrophobic, facilitating the adsorption of biotin-labeled bovine serum albumin (BSA) for incorporation of avidin-labeled epithelial-cell adhesion molecule antibody (anti-EpCAM). In this condition, SiNWAs-PNIPAAm showed higher capture efficiency for EpCAM positive cells (e.g. MCF-7 cells) than EpCAM negative cells (e.g. HeLa cells). Turning off NIR irradiation led to the decrease of temperature to induce the swelling and hydration of PNIPAAm chains, resulting in release of >95% of captured cells. Moreover, SiNWAs-PNIPAAm maintained good cell capture-and-release efficiency over 20 NIR on/off cycles. However, strictly speaking, PNIPAAm is not a bio-inert polymer and its biocompatibility still needs improvement. Therefore, other biocompatible thermoresponsive polymers such as oligo(ethylene glycol)-based (co) polymers [155] and poly(2-oxazoline)s [156] are expected to be used for fabricating photothermal surfaces to regulate cell adhesion and detachment without compromising cell viability. In another work, Huang and co-workers developed a robust platform based on a thermo-responsive gelatin hydrogel embedded with GNRs for separation of cancer cells from blood [149]. The composite hydrogel was prepared by imprinting target cancer cells and incorporating anti-EpCAM on the surface using similar biotin-avidin method, endowing it ability to capture MCF-7 cells efficiently via the synergistic effect between match of cell shape and selective molecular recognition. Under NIR irradiation, the medium temperature increased to 37 °C, leading to the dissolution of gelatin rapidly to release the captured cells. By accurate control of laser area, site-specific release of single MCF-7 cell was achieved. Additionally, efficient capture of cancer cells from lysed or whole blood was realized with 80.7% and 52.0% efficiency, respectively. Using similar method, Xian, Zhang and co-workers fabricated a NIR-switched platform for efficient isolation and downstream analysis of cancer cells [150]. The gelatin mixed with PEG-MoS_2 nanoflakes were firstly modified to ITO surfaces, and then incorporating MUC1 aptamer recognizing MCF-7 cells specifically *via* coupling reaction to achieve the specific capture for cancer cells (Fig. 17b). Importantly, because the conductivities of MoS_2 of cancer cells are relatively close, it was suitable to detect for a small number of cancer cells *in situ* using electrochemical method as MoS_2 could amplify electrical signals. After detection, the captured cancer cells were released from the surface on-demand under NIR irradiation for further analysis and diagnosis.

4.2. Photothermal surfaces for cell sheet harvest

Cell sheets refer to cells growing and proliferating into a confluent sheet, showing great potentials for a wide range of applications such as cell therapy and tissue engineering [157,158]. In the past decades, various materials including biodegradable substrates and stimuli-responsive surfaces have been developed to harvest cell sheets with intact extracellular matrix [159–161]. One of the best studied materials is the PNIPAAm-modified surface due to the thermo-responsive wettability, facilitating the formation and detachment of cell sheets simply by changing temperature [160]. However, this kind of surfaces still has its limitations: (i) low-affinity cells need a longer culture time to form a confluent cell sheet layer, while high-affinity cells need a longer time to detach from the surface; (ii) it is hard to achieve spatial control of detachment to harvest cell sheets with certain shape, limiting the practical applications. Recently, combination of a photothermal substrate and a thermo-responsive "sacrificial layer" becomes an effective strategy for harvest of cell sheets [151]. In this method, cells were seeded on the topmost surface of the sacrificial layer for culture until they formed a confluent layer. Under NIR irradiation, the photothermal substrate produced enough heat to dissolve the sacrificial layer to harvest the cell sheet. Compared with PNIPAAm-based harvest technology, this method has following advantages: (i) the time for harvesting cell sheet (about 5 min) is much less than that using PNIPAAm-modified surfaces (about 30 min); (ii) cell sheets with specific shape could be achieved *via* spatial control of laser; (iii) the viability of detached cell sheet may be well than that treated by PNIPAAm-based substrate due to decreasing temperature would induce certain damage to some sensitive cells.

In recent years, Kim and co-workers developed a series of PEDOT-based photothermal matrixes to achieve non-destructive harvesting of

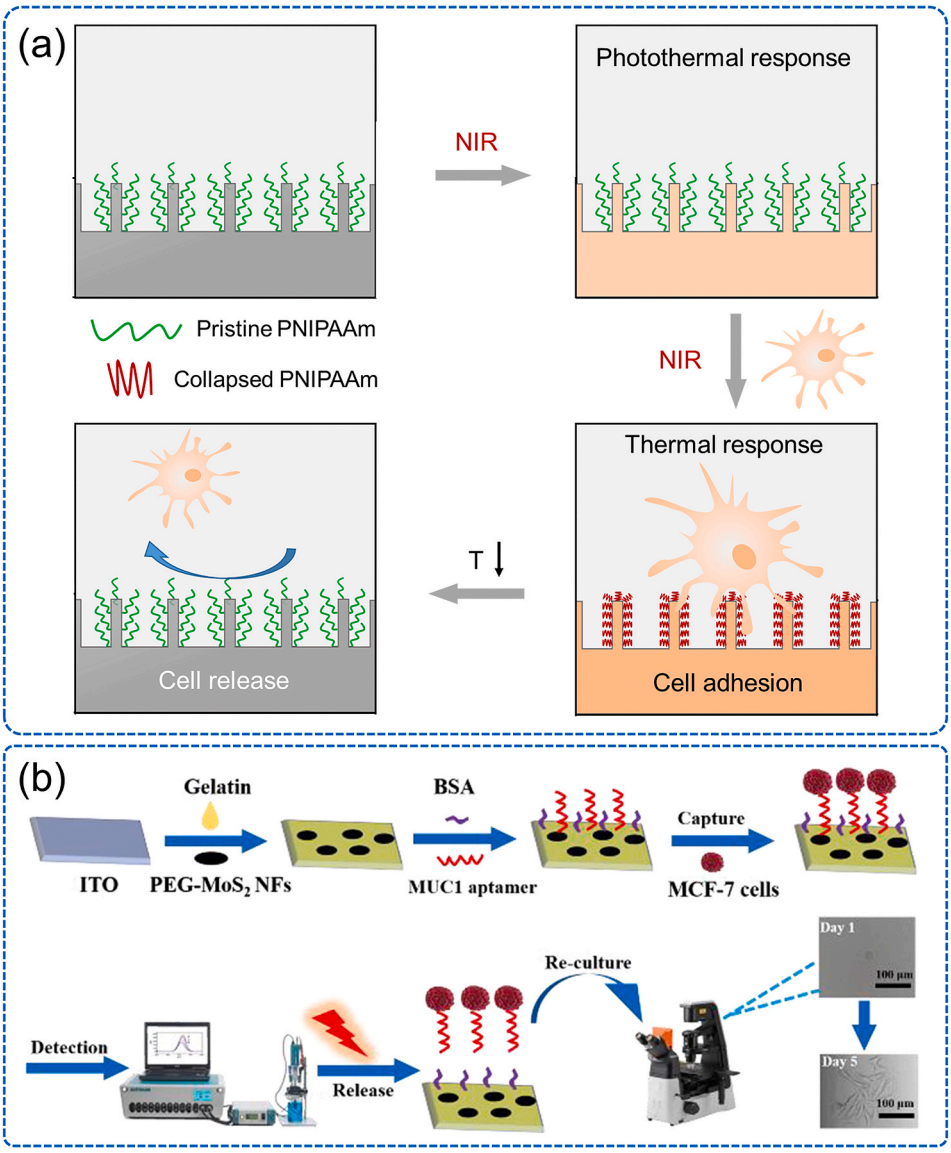

Fig. 17. (a) Scheme of the NIR-controlled cell adhesion and detachment from SiNWAs-PNIPAAm. (b) Scheme of an ITO surface modified with gelatin coating, MoS_2 nanoflowers and MUC1 aptamer for cell capture, *in situ* detection, and release for reculture. Reproduced with permission from Ref. 150. Copyright 2020 American Chemical Society.

various types of cell sheets [151–153]. As shown in Fig. 18a, PEDOT was coated on the polystyrene surface by polymer solution casting, followed by drop casting of a collagen layer with thickness of 14–18 μm [151]. Under NIR irradiation with suitable intensity, the heat produced by PEDOT dissolved the collagen layer, facilitating the harvest of human fibroblast cell sheets non-destructively. In addition, the shapes of the harvested cell sheets could be controlled by changing the shapes of the substrates. Although this approach could harvest cell sheets with diverse shapes, it should be noted that the size of cell sheets was relatively small (<1 cm^2) and it was difficult to achieve multiple harvest of cell sheets. To solve these limitations, on the basis of the above collagen coated PEDOT-modified substrate, they added a patterned optical len (POL), diffracting multiple areas with the same shape on the upper PEDOT-modified substrate as the NIR laser passed through the POL, thus achieving multiple harvest of cell sheets with one dose of NIR light without destroying the cell-cell interactions and compromising cell morphology (Fig. 18b) [152]. Additionally, they used this platform to yield cell sheets with a large area of more than 19 cm^2 and harvested human adipose-derived stem cell (hADSCs) sheets, thereby broadening the applicable types of cell sheets. However, problems still existed that hADSCs were not evenly adhered on the collagens coated PEDOT surfaces and the harvested cell sheets were unstable and showed a broken state after culturing for one day, which might be because the cell-to-cell and cell-to-matrix interactions were relatively poor. In order to harvest a transferrable, free-standing hADSC sheets, they added fibronectin molecules in the cell medium, which are known as cell-adhesion molecules to promote the adhesion and survival of stem cells [153]. A confluent layer of hADSCs formed on the collage coated PEDOT surface after culturing for one day and their proliferation rate was significantly higher than that without fibronectin molecules. Most noteworthy is that the free-standing hADSCs sheet with an area of 122.6 mm^2 was transferred and attached onto the chronic wound of genetically diabetic *db/db* mice. The wound healing effect was significantly better than that using injected cells, exhibiting the potential application in skin reproduction and organ regeneration.

Although intact cell sheets could be produced by using the PEDOT-coated surfaces mentioned above, there are still a lot of problems in clinical trial. For example, in some elaborate clinical trials, obtaining a unified cell sheet operation plays an important role in promoting an ordered, consistent and reproducible production. In order to harvest cell

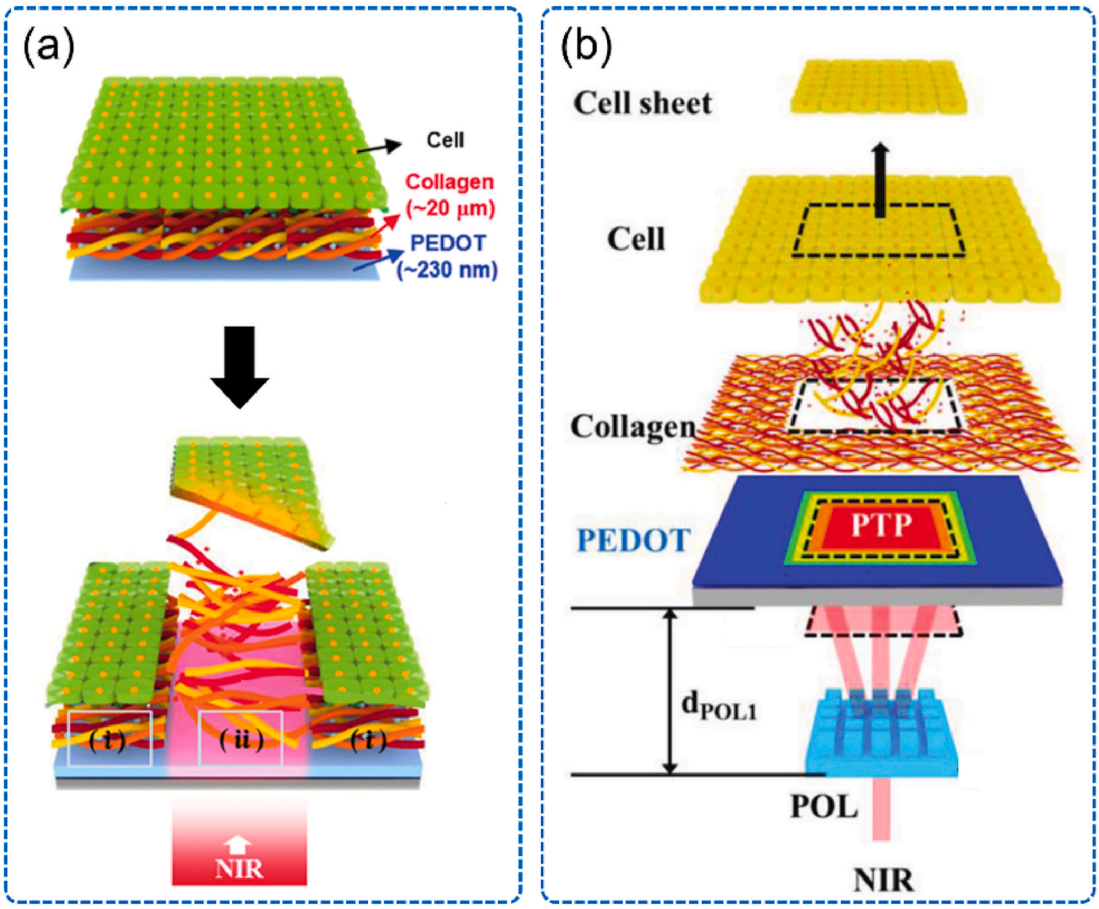

Fig. 18. (a) Scheme of a collagen-coated PEDOT surface for harvest of cell sheets by dissolving the collagen layer under NIR irradiation. Reproduced with permission from Ref. 151. Copyright 2015 John Wiley and Sons. (b) Schematic illustration of harvest of a square type of cell sheet from a nonpatterned PEDOT substrate using an optical setup composed of an NIR laser and patterned optical lens. Reproduced with permission from Ref. 152. Copyright 2017 John Wiley and Sons.

sheets along a predetermined direction, Lu and co-workers fabriated a PEDOT film with gradient thickness, which could guide guides detachment of cell sheets accurately by thermally-induced collagen dissociation (Fig. 19a) [154]. Under identical NIR irradiation, the heating rate at the thicker side of the PEDOT film was larger than that at the thinner side, thus the dissociation of coated collage layer as well as

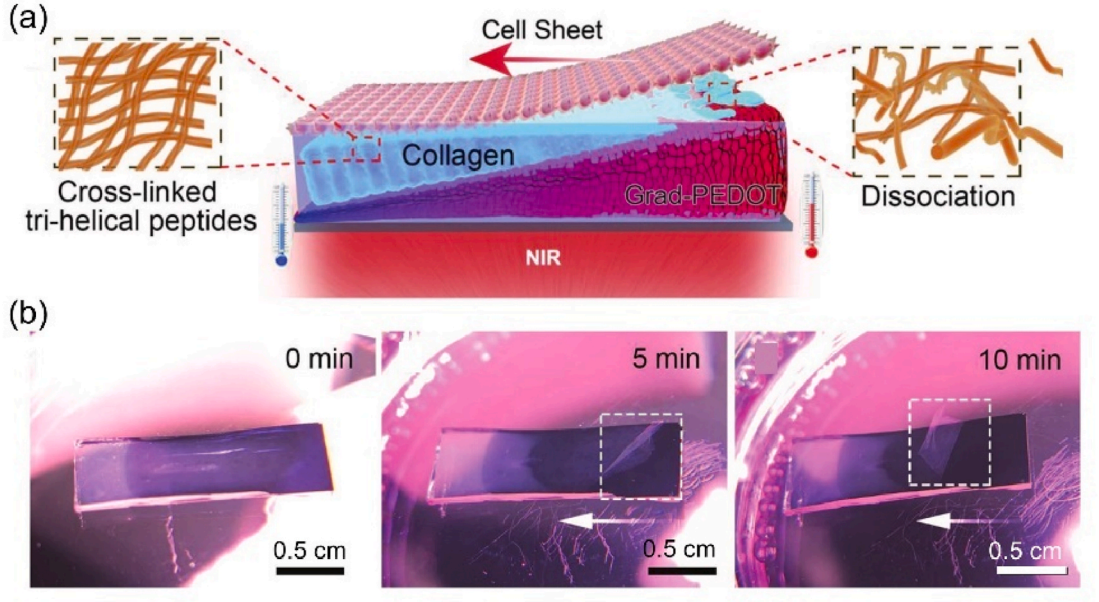

Fig. 19. (a) Schematic illustration of a PEDOT film with gradient thickness for guiding cell sheet detachment accurately. (b) Optical images of precisely directed detachment of a fibroblast cell sheet at 0, 5, and 10 min. Reproduced with permission from Ref. 154. Copyright 2019 John Wiley and Sons.

the detachment of fibroblast cell sheet proceeded along the decrease direction of PEDOT film thickness (Fig. 19b). Using this method, it is possible to harvest cell sheet in a controlled manner to obtain cell sheets with predetermined direction.

5. Summary and future perspectives

During the past decade, photothermal scaffolds/surfaces have attracted great interest in regulating cell behaviors by the generated heat under NIR irradiation. In this review, we systematically summarize recent achievements in this promising area and discuss the respective characteristics. As an emerging platform, the interaction between photothermal scaffolds/surfaces and the attached cells can be adjusted by simply adjusting the NIR laser intensity to achieve specific biological phenomenon (e.g. the intensive heat produced under NIR irradiation with high intensity causes tumor ablation, and moderate heat produced under NIR irradiation with relatively low intensity increases membrane permeability of attached cells to promote the delivery of exogenous molecules to cells or changes the surface properties to achieve controlled cell adhesion-detachment), which shows great potential in cancer treatment, tissue engineering, immune therapy, gene editing and other biomedical applications.

Although considerable progress has been made, there are still some remaining challenges that need to be solved in future. (i) Currently, the penetration depth of NIR light is still limited, which restricts the treatment effect to deep tumors. The latest research in optical imaging shows that longer-wavelength NIR light in the NIR-II window (1000–1700 nm) [162–164] has a higher potential for depth imaging than NIR light in NIR-I window (700–900 nm). Therefore, applying PTAs in response to the NIR-II window for fabrication of photothermal scaffolds/surfaces has great potential in many biological applications. Additionally, exploitation of PTAs with higher photothermal effect and absorption coefficient may also be helpful to solve this limitation. (ii) At present, photothermal scaffolds/surfaces prepared by freeze-drying, mixing methods, electrospinning or 3D printing technique either have simple preparation but poor reproducibility and are not easy to finely control, or have good repeatability but require expensive equipment and complex technology. For practical applications, it is of great significance to develop photothermal scaffolds/surfaces integrating good repeatability, high precision, simple preparation method and easy to expand production. (iii) Most current photothermal scaffolds/surfaces used for tumor ablation are irradiated by high-intensity NIR laser, which may cause large damage to normal cells and healthy tissues. Therefore, it is still necessary to combine PTT and other therapeutic methods such as chemotherapy and photodynamic therapy to reduce the NIR light intensity for avoiding damage to normal cells, while maintaining effective tumor ablation. (iv) Although considerable progress has been made for intracellular delivery using photothermal scaffolds/surfaces, some important issues need to be addressed. One is the mechanism of membrane disruption should be further explored to provide the theoretical basis for intracellular delivery. Another is that the current intracellular delivery using photothermal scaffolds/surfaces is only carried out in laboratory, however, issues related to scale-up and cost should also be considered for future practical applications. (v) Because biological systems are dynamic, it is of significance for designing dynamic surfaces whose properties such as stiffness can change under NIR irradiation to control cell behaviors beyond adhesion. Moreover, the current platforms are still limited in response to multiple stimuli, combining light stimulus and/or other stimuli together and using different response pairs in turn will have outstanding advantages in regulating cell behaviors.

In summary, this review aims to emphasize the recent developments of regulation of cell behaviors by photothermal scaffolds/surfaces as well as their exploration for tumor therapy, cell engineering, and tissue engineering. With the development of cell biology, biomaterial technology and processing and manufacturing technology, it is foreseen that these materials will gradually solve these current limitations and continue to open up new possibilities for precisely controlling cell behaviors and determining cell fates.

CRediT authorship contribution statement

Yangcui Qu: Writing - original draft. **Kunyan Lu:** Writing - original draft. **Yanjun Zheng:** Writing - original draft. **Chaobo Huang:** Writing - review & editing. **Guannan Wang:** Writing - review & editing, Funding acquisition. **Yanxia Zhang:** Writing - review & editing, Funding acquisition. **Qian Yu:** Conceptualization, Writing - review & editing, Funding acquisition, Project administration.

Declaration of competing interest

The authors declare no conflicts of interest.

Acknowledgments

This work was supported by the National Natural Science Foundation of China (21774086 and 81671742), the Natural Science Foundation of Jiangsu Province (BK20180093), the Suzhou Municipal Science and Technology Foundation (SYS2018026), and the Start-Up Grant of Jining Medical University (600910001).

References

[1] S.A. Morris, G.Q. Daley, A blueprint for engineering cell fate: current technologies to reprogram cell identity, Cell Res. 23 (2013) 33–48, https://doi.org/10.1038/cr.2013.1.
[2] W. Li, Z. Yan, J. Ren, X. Qu, Manipulating cell fate: dynamic control of cell behaviors on functional platforms, Chem. Soc. Rev. 47 (2018) 8639–8684, https://doi.org/10.1039/c8cs00053k.
[3] Y. Ma, X. Tian, L. Liu, J. Pan, G. Pan, Dynamic synthetic biointerfaces: from reversible chemical interactions to tunable biological effects, Acc. Chem. Res. 52 (2019) 1611–1622, https://doi.org/10.1021/acs.accounts.8b00604.
[4] A. Tay, N. Melosh, Nanostructured materials for intracellular cargo delivery, Acc. Chem. Res. 52 (2019) 2462–2471, https://doi.org/10.1021/acs.accounts.9b00272.
[5] Y. Hou, L. Yu, W. Xie, L.C. Camacho, M. Zhang, Z. Chu, Q. Wei, R. Haag, Surface roughness and substrate stiffness synergize to drive cellular mechanoresponse, Nano Lett. 20 (2020) 748–757, https://doi.org/10.1021/acs.nanolett.9b04761.
[6] M. Ermis, E. Antmen, V. Hasirci, Micro and nanofabrication methods to control cell-substrate interactions and cell behavior: a review from the tissue engineering perspective, Bioact. Mater. 3 (2018) 355–369, https://doi.org/10.1016/j.bioactmat.2018.05.005.
[7] N. Li, Y. Wang, D. Zhao, B. Deng, X. Fan, X. He, Thermal reversal surface with "sticky tentacle" for modulating initial cell adhesion and detachment, Mater. Des. 199 (2021) 109402, https://doi.org/10.1016/j.matdes.2020.109402.
[8] T. Grosges, D. Barchiesi, Gold nanoparticles as a photothermal agent in cancer therapy: the thermal ablation characteristic length, Molecules 23 (2018) 1316, https://doi.org/10.3390/molecules23061316.
[9] Z. Ashikbayeva, D. Tosi, D. Balmassov, E. Schena, P. Saccomandi, V. Inglezakis, Application of nanoparticles and nanomaterials in thermal ablation therapy of cancer, Nanomaterials 9 (2019) 1195, https://doi.org/10.3390/nano9091195.
[10] L. Sun, R.A. Bockmann, Membrane phase transition during heating and cooling: molecular insight into reversible melting, Eur. Biophys. J. 47 (2018) 151–164, https://doi.org/10.1007/s00249-017-1237-3.
[11] A.K. Fajrial, X. Ding, Advanced nanostructures for cell membrane poration, Nanotechnology 30 (2019) 264002, https://doi.org/10.1088/1361-6528/ab096b.
[12] M. Sponchioni, U. Capasso Palmiero, D. Moscatelli, Thermo-responsive polymers: applications of smart materials in drug delivery and tissue engineering, Mater. Sci. Eng. C 102 (2019) 589–605, https://doi.org/10.1016/j.msec.2019.04.069.
[13] Z. Lv, S. He, Y. Wang, X. Zhu, Noble metal nanomaterials for NIR-triggered photothermal therapy in cancer, Adv. Healthc. Mater. 10 (2021) 2001806, https://doi.org/10.1002/adhm.202001806.
[14] X. Huang, W. Zhang, G. Guan, G. Song, R. Zou, J. Hu, Design and functionalization of the NIR-responsive photothermal semiconductor nanomaterials for cancer theranostics, Acc. Chem. Res. 50 (2017) 2529–2538, https://doi.org/10.1021/acs.accounts.7b00294.
[15] Q. Zhang, W. Xu, X. Wang, Carbon nanocomposites with high photothermal conversion efficiency, Sci. China Mater. 61 (2018) 905–914, https://doi.org/10.1007/s40843-018-9250-x.
[16] Y. Wang, H. Zhang, Z. Wang, L. Feng, Photothermal conjugated polymers and their biological applications in imaging and therapy, ACS Appl. Polym. Mater. 2 (2020) 4222–4240, https://doi.org/10.1021/acsapm.0c00672.
[17] G. Ratheesh, J.R. Venugopal, A. Chinappan, H. Ezhilarasu, A. Sadiq, S. Ramakrishna, 3D fabrication of polymeric scaffolds for regenerative therapy,

ACS Biomater. Sci. Eng. 3 (2017) 1175–1194, https://doi.org/10.1021/acsbiomaterials.6b00370.
[18] M. Mabrouk, H.H. Beherei, D.B. Das, Recent progress in the fabrication techniques of 3D scaffolds for tissue engineering, Mater. Sci. Eng. C 110 (2020) 110716, https://doi.org/10.1016/j.msec.2020.110716.
[19] G. Chen, Y. Cao, Y. Tang, X. Yang, Y. Liu, D. Huang, Y. Zhang, C. Li, Q. Wang, Advanced near-infrared light for monitoring and modulating the spatiotemporal dynamics of cell functions in living systems, Adv. Sci. 7 (2020) 1903783, https://doi.org/10.1002/advs.201903783.
[20] T. Wei, Q. Yu, H. Chen, Responsive and synergistic antibacterial coatings: fighting against bacteria in a smart and effective way, Adv. Healthc. Mater. 8 (2019) 1801381, https://doi.org/10.1002/adhm.201801381.
[21] Y. Ren, H. Liu, X. Liu, Y. Zheng, Z. Li, C. Li, K.W.K. Yeung, S. Zhu, Y. Liang, Z. Cui, S. Wu, Photoresponsive materials for antibacterial applications, Cell Rep. Phys. Sci. 1 (2020) 100245, https://doi.org/10.1016/j.xcrp.2020.100245.
[22] Y. Zou, Y. Zhang, Q. Yu, H. Chen, Photothermal bactericidal surfaces: killing bacteria using light instead of biocides, Biomater. Sci. 9 (2021) 10–22, https://doi.org/10.1039/d0bm00617c.
[23] Y. Zou, Y. Zhang, Q. Yu, H. Chen, Dual-function antibacterial surfaces to resist and kill bacteria: painting a picture with two brushes simultaneously, J. Mater. Sci. Technol. 70 (2021) 24–38, https://doi.org/10.1016/j.jmst.2020.07.028.
[24] M. Yang, J. Li, P. Gu, X. Fan, The application of nanoparticles in cancer immunotherapy: targeting tumor microenvironment, Bioact. Mater. 6 (2021) 1973–1987, https://doi.org/10.1016/j.bioactmat.2020.12.010.
[25] R.A. Ward, S. Fawell, N. Floc'h, V. Flemington, D. McKerrecher, P.D. Smith, Challenges and opportunities in cancer drug resistance, Chem. Rev. 121 (2021) 3297–3351, https://doi.org/10.1021/acs.chemrev.0c00383.
[26] C.M. Hartshorn, M.S. Bradbury, G.M. Lanza, A.E. Nel, J. Rao, A.Z. Wang, U. B. Wiesner, L. Yang, P. Grodzinski, Nanotechnology strategies to advance outcomes in clinical cancer care, ACS Nano 12 (2018) 24–43, https://doi.org/10.1021/acsnano.7b05108.
[27] L. Zou, H. Wang, B. He, L. Zeng, T. Tan, H. Cao, X. He, Z. Zhang, S. Guo, Y. Li, Current approaches of photothermal therapy in treating cancer metastasis with nanotherapeutics, Theranostics 6 (2016) 762–772, https://doi.org/10.7150/thno.14988.
[28] J.-J. Hu, Y.-J. Cheng, X.-Z. Zhang, Recent advances in nanomaterials for enhanced photothermal therapy of tumors, Nanoscale 10 (2018) 22657–22672, https://doi.org/10.1039/c8nr07627h.
[29] A.C.V. Doughty, A.R. Hoover, E. Layton, C.K. Murray, E.W. Howard, W.R. Chen, Nanomaterial applications in photothermal therapy for cancer, Materials 12 (2019) 779, https://doi.org/10.3390/ma12050779.
[30] S. Liu, X. Pan, H. Liu, Two-dimensional nanomaterials for photothermal therapy, Angew. Chem. Int. Ed. 59 (2020) 5890–5900, https://doi.org/10.1002/anie.201911477.
[31] D.S. Salem, S.F. Hegazy, S.S.A. Obayya, Nanogold-loaded chitosan nanocomposites for pH/light-responsive drug release and synergistic chemo-photothermal cancer therapy, Colloid Interface Sci. Commun. 41 (2021) 100361, https://doi.org/10.1016/j.colcom.2021.100361.
[32] J. Zhang, J. Li, S. Chen, N. Kawazoe, G. Chen, Preparation of gelatin/Fe_3O_4 composite scaffolds for enhanced and repeatable cancer cell ablation, J. Mater. Chem. B 4 (2016) 5664–5672, https://doi.org/10.1039/c6tb01543c.
[33] J. Zhang, J. Li, N. Kawazoe, G. Chen, Composite scaffolds of gelatin and gold nanoparticles with tunable size and shape for photothermal cancer therapy, J. Mater. Chem. B 5 (2017) 245–253, https://doi.org/10.1039/c6tb02872a.
[34] J. Zhang, J. Li, X. Wang, N. Kawazoe, G. Chen, Targeting ligand-functionalized photothermal scaffolds for cancer cell capture and in situ ablation, Biomater. Sci. 5 (2017) 2276–2284, https://doi.org/10.1039/C7BM00639J.
[35] X. Wang, N. Kawazoe, G. Chen, Interaction of immune cells and tumor cells in gold nanorod-gelatin composite porous scaffolds, Nanomaterials 9 (2019) 1367, https://doi.org/10.3390/nano9101367.
[36] J. Shao, C. Ruan, H. Xie, Z. Li, H. Wang, P.K. Chu, X.-F. Yu, Black-phosphorus-incorporated hydrogel as a sprayable and biodegradable photothermal platform for postsurgical treatment of cancer, Adv. Sci. 5 (2018) 1700848, https://doi.org/10.1002/advs.201700848.
[37] X. Wang, C. Wang, X. Wang, Y. Wang, Q. Zhang, Y. Cheng, A polydopamine nanoparticle-knotted poly(ethylene glycol) hydrogel for on-demand drug delivery and chemo-photothermal therapy, Chem. Mater. 29 (2017) 1370–1376, https://doi.org/10.1021/acs.chemmater.6b05192.
[38] A. GhavamiNejad, M. SamariKhalaj, L.E. Aguilar, C.H. Park, C.S. Kim, pH/NIR light-controlled multidrug release *via* a mussel-inspired nanocomposite hydrogel for chemo-photothermal cancer therapy, Sci. Rep. 6 (2016) 33594, https://doi.org/10.1038/srep33594.
[39] Y. Wu, K. Wang, S. Huang, C. Yang, M. Wang, Near-infrared light-responsive semiconductor polymer composite hydrogels: spatial/temporal-controlled release via a photothermal "sponge" effect, ACS Appl. Mater. Interfaces 9 (2017) 13602–13610, https://doi.org/10.1021/acsami.7b01016.
[40] Q. Li, J. Wen, C. Liu, Y. Jia, Y. Wu, Y. Shan, Z. Qian, J. Liao, Graphene-nanoparticle-based self-healing hydrogel in preventing postoperative recurrence of breast cancer, ACS Biomater. Sci. Eng. 5 (2019) 768–779, https://doi.org/10.1021/acsbiomaterials.8b01475.
[41] X. Wang, B. Ma, J. Xue, J. Wu, J. Chang, C. Wu, Defective black nano-titania thermogels for cutaneous tumor-induced therapy and healing, Nano Lett. 19 (2019) 2138–2147, https://doi.org/10.1021/acs.nanolett.9b00367.
[42] X. Wang, J. Zhang, J. Li, Y. Chen, Y. Chen, N. Kawazoe, G. Chen, Bifunctional scaffolds for the photothermal therapy of breast tumor cells and adipose tissue regeneration, J. Mater. Chem. B 6 (2018) 7728–7736, https://doi.org/10.1039/c8tb02325e.
[43] D. Li, W. Nie, L. Chen, D. McCoul, D. Liu, X. Zhang, Y. Ji, B. Yu, C. He, Self-assembled hydroxyapatite-graphene scaffold for photothermal cancer therapy and bone regeneration, J. Biomed. Nanotechnol. 14 (2018) 2003–2017, https://doi.org/10.1166/jbn.2018.2646.
[44] H. Ma, Q. Zhou, J. Chang, C. Wu, Grape seed-inspired smart hydrogel scaffolds for melanoma therapy and wound healing, ACS Nano 13 (2019) 4302–4311, https://doi.org/10.1021/acsnano.8b09496.
[45] J. Shao, H. Xie, H. Wang, W. Zhou, Q. Luo, X.F. Yu, P.K. Chu, 2D material-based nanofibrous membrane for photothermal cancer therapy, ACS Appl. Mater. Interfaces 10 (2018) 1155–1163, https://doi.org/10.1021/acsami.7b17117.
[46] N. Mauro, C. Scialabba, G. Pitarresi, G. Giammona, Enhanced adhesion and *in situ* photothermal ablation of cancer cells in surface-functionalized electrospun microfiber scaffold with graphene oxide, Int. J. Pharm. 526 (2017) 167–177, https://doi.org/10.1016/j.ijpharm.2017.04.045.
[47] Y. Chen, Z. Hou, B. Liu, S. Huang, C. Li, J. Lin, DOX-Cu_9S_5@mSiO_2-PG composite fibers for orthotopic synergistic chemo- and photothermal tumor therapy, Dalton Trans. 44 (2015) 3118–3127, https://doi.org/10.1039/c4dt03113j.
[48] F.O. Obiweluozor, G.A. Emechebe, A.P. Tiwari, J.Y. Kim, C.H. Park, C.S. Kim, Short duration cancer treatment: inspired by a fast bio-resorbable smart nano-fiber device containing NIR lethal polydopamine nanospheres for effective chemo-photothermal cancer therapy, Int. J. Nanomed. 13 (2018) 6375–6390, https://doi.org/10.2147/ijn.S180970.
[49] A.P. Tiwari, T.I. Hwang, J.M. Oh, B. Maharjan, S. Chun, B.S. Kim, M.K. Joshi, C. H. Park, C.S. Kim, pH/NIR-responsive polypyrrole-functionalized fibrous localized drug-delivery platform for synergistic cancer therapy, ACS Appl. Mater. Interfaces 10 (2018) 20256–20270, https://doi.org/10.1021/acsami.7b17664.
[50] A.P. Tiwari, D.P. Bhattarai, B. Maharjan, S.W. Ko, H.Y. Kim, C.H. Park, C.S. Kim, Polydopamine-based implantable multifunctional nanocarpet for highly efficient photothermal-chemo therapy, Sci. Rep. 9 (2019) 2943, https://doi.org/10.1038/s41598-019-39457-y.
[51] D. Cen, Z. Wan, Y. Fu, H. Pan, J. Xu, Y. Wang, Y. Wu, X. Li, X. Cai, Implantable fibrous 'patch' enabling preclinical chemo-photothermal tumor therapy, Colloids Surf. B Biointerfaces 192 (2020) 111005, https://doi.org/10.1016/j.colsurfb.2020.111005.
[52] X. Wang, F. Lv, T. Li, Y. Han, Z. Yi, M. Liu, J. Chang, C. Wu, Electrospun micropatterned nanocomposites incorporated with Cu_2S nanoflowers for skin tumor therapy and wound healing, ACS Nano 11 (2017) 11337–11349, https://doi.org/10.1021/acsnano.7b05858.
[53] Q. Yu, Y. Han, T. Tian, Q. Zhou, Z. Yi, J. Chang, C. Wu, Chinese sesame stick-inspired nano-fibrous scaffolds for tumor therapy and skin tissue reconstruction, Biomaterials 194 (2019) 25–35, https://doi.org/10.1016/j.biomaterials.2018.12.012.
[54] Q. Yu, Y. Han, X. Wang, C. Qin, D. Zhai, Z. Yi, J. Chang, Y. Xiao, C. Wu, Copper silicate hollow microspheres-incorporated scaffolds for chemo-photothermal therapy of melanoma and tissue healing, ACS Nano 12 (2018) 2695–2707, https://doi.org/10.1021/acsnano.7b08928.
[55] H. Ma, C. Jiang, D. Zhai, Y. Luo, Y. Chen, F. Lv, Z. Yi, Y. Deng, J. Wang, J. Chang, C. Wu, A bifunctional biomaterial with photothermal effect for tumor therapy and bone regeneration, Adv. Funct. Mater. 26 (2016) 1197–1208, https://doi.org/10.1002/adfm.201504142.
[56] H. Ma, J. Luo, Z. Sun, L. Xia, M. Shi, M. Liu, J. Chang, C. Wu, 3D printing of biomaterials with mussel-inspired nanostructures for tumor therapy and tissue regeneration, Biomaterials 111 (2016) 138–148, https://doi.org/10.1016/j.biomaterials.2016.10.005.
[57] X. Wang, T. Li, H. Ma, D. Zhai, C. Jiang, J. Chang, J. Wang, C. Wu, A 3D-printed scaffold with MoS_2 nanosheets for tumor therapy and tissue regeneration, NPG Asia Mater. 9 (2017), https://doi.org/10.1038/am.2017.47 e376-e376.
[58] H. Wang, X. Zeng, L. Pang, H. Wang, B. Lin, Z. Deng, E.L.X. Qi, N. Miao, D. Wang, P. Huang, H. Hu, J. Li, Integrative treatment of anti-tumor/bone repair by combination of MoS_2 nanosheets with 3D printed bioactive borosilicate glass scaffolds, Chem. Eng. J. 396 (2020) 125081, https://doi.org/10.1016/j.cej.2020.125081.
[59] S. Fu, H. Hu, J. Chen, Y. Zhu, S. Zhao, Silicone resin derived larnite/C scaffolds *via* 3D printing for potential tumor therapy and bone regeneration, Chem. Eng. J. 382 (2020) 122928, https://doi.org/10.1016/j.cej.2019.122928.
[60] H. Zhuang, R. Lin, Y. Liu, M. Zhang, D. Zhai, Z. Huan, C. Wu, Three-dimensional-printed bioceramic scaffolds with osteogenic activity for simultaneous photo/magnetothermal therapy of bone tumors, ACS Biomater. Sci. Eng. 5 (2019) 6725–6734, https://doi.org/10.1021/acsbiomaterials.9b01095.
[61] Q. Yang, H. Yin, T. Xu, D. Zhu, J. Yin, Y. Chen, X. Yu, J. Gao, C. Zhang, Y. Chen, Y. Gao, Engineering 2D mesoporous Silica@MXene-integrated 3D-printing scaffolds for combinatory osteosarcoma therapy and No-augmented bone regeneration, Small 16 (2020) 1906814, https://doi.org/10.1002/smll.201906814.
[62] B. Yang, J. Yin, Y. Chen, S. Pan, H. Yao, Y. Gao, J. Shi, 2D-Black-Phosphorus-Reinforced 3D-printed scaffolds: a stepwise countermeasure for osteosarcoma, Adv. Mater. 30 (2018) 1705611, https://doi.org/10.1002/adma.201705611.
[63] S. Pan, J. Yin, L. Yu, C. Zhang, Y. Zhu, Y. Gao, Y. Chen, 2D MXene-integrated 3D-printing scaffolds for augmented osteosarcoma phototherapy and accelerated tissue reconstruction, Adv. Sci. 7 (2020) 1901511, https://doi.org/10.1002/advs.201901511.
[64] W. Dang, T. Li, B. Li, H. Ma, D. Zhai, X. Wang, J. Chang, Y. Xiao, J. Wang, C. Wu, A bifunctional scaffold with $CuFeSe_2$ nanocrystals for tumor therapy and bone

reconstruction, Biomaterials 160 (2018) 92–106, https://doi.org/10.1016/j.biomaterials.2017.11.020.
[65] Y. Liu, T. Li, H. Ma, D. Zhai, C. Deng, J. Wang, S. Zhuo, J. Chang, C. Wu, 3D-Printed scaffolds with bioactive elements-induced photothermal effect for bone tumor therapy, Acta Biomater. 73 (2018) 531–546, https://doi.org/10.1016/j.actbio.2018.04.014.
[66] W. Dang, B. Ma, Z. Huan, R. Lin, X. Wang, T. Li, J. Wu, N. Ma, H. Zhu, J. Chang, C. Wu, Lab_6 surface chemistry-reinforced scaffolds for treating bone tumors and bone defects, Appl. Mater. Today 16 (2019) 42–55, https://doi.org/10.1016/j.apmt.2019.04.015.
[67] M. Sepantafar, R. Maheronnaghsh, H. Mohammadi, F. Radmanesh, M.M. Hasani-Sadrabadi, M. Ebrahimi, H. Baharvand, Engineered hydrogels in cancer therapy and diagnosis, Trends Biotechnol. 35 (2017) 1074–1087, https://doi.org/10.1016/j.tibtech.2017.06.015.
[68] H. Zhang, T. Fan, W. Chen, Y. Li, B. Wang, Recent advances of two-dimensional materials in smart drug delivery nano-systems, Bioact. Mater. 5 (2020) 1071–1086, https://doi.org/10.1016/j.bioactmat.2020.06.012.
[69] Z. Sun, C. Song, C. Wang, Y. Hu, J. Wu, Hydrogel-based controlled drug delivery for cancer treatment: a review, Mol. Pharmaceut. 17 (2020) 373–391, https://doi.org/10.1021/acs.molpharmaceut.9b01020.
[70] F. Li, M. Wang, H. Cai, Y. He, H. Xu, Y. Liu, Y. Zhao, Nondestructive capture, release, and detection of circulating tumor cells with cystamine-mediated folic acid decorated magnetic nanospheres, J. Mater. Chem. B 8 (2020) 9971–9979, https://doi.org/10.1039/d0tb01091j.
[71] F. Ding, X. Gao, X. Huang, H. Ge, M. Xie, J. Qian, J. Song, Y. Li, X. Zhu, C. Zhang, Polydopamine-coated nucleic acid nanogel for siRNA-mediated low-temperature photothermal therapy, Biomaterials 245 (2020) 119976, https://doi.org/10.1016/j.biomaterials.2020.119976.
[72] J. Dai, Y. Wang, D. Wu, F. Wan, Y. Lu, N. Kong, X. Li, J. Gong, S. Ling, Y. Yao, Biointerface mediates cytoskeletal rearrangement of pancreatic cancer cell and modulates its drug sensitivity, Colloid Interface Sci. Commun. 35 (2020) 100250, https://doi.org/10.1016/j.colcom.2020.100250.
[73] E. Boedtkjer, S.F. Pedersen, The acidic tumor microenvironment as a driver of cancer, Annu. Rev. Physiol. 82 (2020) 103–126, https://doi.org/10.1146/annurev-physiol-021119-034627.
[74] Y. Zhao, B.Q. Chen, R.K. Kankala, S.B. Wang, A.Z. Chen, Recent advances in combination of copper chalcogenide-based photothermal and reactive oxygen species-related therapies, ACS Biomater. Sci. Eng. 6 (2020) 4799–4815, https://doi.org/10.1021/acsbiomaterials.0c00830.
[75] P.-Y. Xu, X. Zheng, R.K. Kankala, S.-B. Wang, A.-Z. Chen, Advances in indocyanine green-based codelivery nanoplatforms for combinatorial therapy, ACS Biomater. Sci. Eng. 7 (2021) 939–962, https://doi.org/10.1021/acsbiomaterials.0c01644.
[76] J.K. Cullen, J.L. Simmons, P.G. Parsons, G.M. Boyle, Topical treatments for skin cancer, Adv. Drug Deliv. Rev. 153 (2020) 54–64, https://doi.org/10.1016/j.addr.2019.11.002.
[77] C. Bastiancich, J. Bianco, K. Vanvarenberg, B. Ucakar, N. Joudiou, B. Gallez, G. Bastiat, F. Lagarce, V. Preat, F. Danhier, Injectable nanomedicine hydrogel for local chemotherapy of glioblastoma after surgical resection, J. Contr. Release 264 (2017) 45–54, https://doi.org/10.1016/j.jconrel.2017.08.019.
[78] A. Raslan, L. Saenz Del Burgo, J. Ciriza, J.L. Pedraz, Graphene oxide and reduced graphene oxide-based scaffolds in regenerative medicine, Int. J. Pharm. 580 (2020) 119226, https://doi.org/10.1016/j.ijpharm.2020.119226.
[79] W. Nie, C. Peng, X. Zhou, L. Chen, W. Wang, Y. Zhang, P.X. Ma, C. He, Three-dimensional porous scaffold by self-assembly of reduced graphene oxide and nano-hydroxyapatite composites for bone tissue engineering, Carbon 116 (2017) 325–337, https://doi.org/10.1016/j.carbon.2017.02.013.
[80] Y. Wang, W. Zhang, C. Gong, B. Liu, Y. Li, L. Wang, Z. Su, G. Wei, Recent advances in the fabrication, functionalization, and bioapplications of peptide hydrogels, Soft Matter 16 (2020) 10029–10045, https://doi.org/10.1039/d0sm00966k.
[81] S. Chen, S.K. Boda, S.K. Batra, X. Li, J. Xie, Emerging roles of electrospun nanofibers in cancer research, Adv. Healthc. Mater. 7 (2018) 1701024, https://doi.org/10.1002/adhm.201701024.
[82] R. Contreras-Caceres, L. Cabeza, G. Perazzoli, A. Diaz, J.M. Lopez-Romero, C. Melguizo, J. Prados, Electrospun nanofibers: recent applications in drug delivery and cancer therapy, Nanomaterials 9 (2019) 656, https://doi.org/10.3390/nano9040656.
[83] Y. Chen, M. Shafiq, M. Liu, Y. Morsi, X. Mo, Advanced fabrication for electrospun three-dimensional nanofiber aerogels and scaffolds, Bioact. Mater. 5 (2020) 963–979, https://doi.org/10.1016/j.bioactmat.2020.06.023.
[84] W. Fan, B. Yung, P. Huang, X. Chen, Nanotechnology for multimodal synergistic cancer therapy, Chem. Rev. 117 (2017) 13566–13638, https://doi.org/10.1021/acs.chemrev.7b00258.
[85] S. Gai, G. Yang, P. Yang, F. He, J. Lin, D. Jin, B. Xing, Recent advances in functional nanomaterials for light-triggered cancer therapy, Nano Today 19 (2018) 146–187, https://doi.org/10.1016/j.nantod.2018.02.010.
[86] J. Xiao, S. Chen, J. Yi, H. Zhang, G.A. Ameer, A cooperative copper metal-organic framework-hydrogel system improves wound healing in diabetes, Adv. Funct. Mater. 27 (2017) 1604872, https://doi.org/10.1002/adfm.201604872.
[87] T. Tian, C. Wu, J. Chang, Preparation and in vitro osteogenic, angiogenic and antibacterial properties of cuprorivaite ($CaCuSi_4O_{10}$, cup) bioceramics, RSC Adv. 6 (2016) 45840–45849, https://doi.org/10.1039/c6ra08145b.
[88] A. Alves, R.A. Sousa, R.L. Reis, Processing of degradable ulvan 3D porous structures for biomedical applications, J. Biomed. Mater. Res. 101 (2013) 998–1006, https://doi.org/10.1002/jbm.a.34403.
[89] J.K. Placone, A.J. Engler, Recent advances in extrusion-based 3D printing for biomedical applications, Adv. Healthc. Mater. 7 (2018) 1701161, https://doi.org/10.1002/adhm.201701161.
[90] G. Palmara, F. Frascella, I. Roppolo, A. Chiappone, A. Chiado, Functional 3D printing: approaches and bioapplications, Biosens. Bioelectron. 175 (2021) 112849, https://doi.org/10.1016/j.bios.2020.112849.
[91] M.V. Varma, B. Kandasubramanian, S.M. Ibrahim, 3D printed scaffolds for biomedical applications, Mater. Chem. Phys. 255 (2020) 123642, https://doi.org/10.1016/j.matchemphys.2020.123642.
[92] B. Joseph, S.V. K, C. Sabu, N. Kalarikkal, S. Thomas, Cellulose nanocomposites: fabrication and biomedical applications, J. Bioresour. Bioprod. 5 (2020) 223–237, https://doi.org/10.1016/j.jobab.2020.10.001.
[93] C. Wang, W. Huang, Y. Zhou, L. He, Z. He, Z. Chen, X. He, S. Tian, J. Liao, B. Lu, Y. Wei, M. Wang, 3D printing of bone tissue engineering scaffolds, Bioact. Mater. 5 (2020) 82–91, https://doi.org/10.1016/j.bioactmat.2020.01.004.
[94] H. Ma, C. Feng, J. Chang, C. Wu, 3D-Printed bioceramic scaffolds: from bone tissue engineering to tumor therapy, Acta Biomater. 79 (2018) 37–59, https://doi.org/10.1016/j.actbio.2018.08.026.
[95] Z.C. Eckel, C. Zhou, J.H. Martin, A.J. Jacobsen, W.B. Carter, T.A. Schaedler, Additive manufacturing of polymer-derived ceramics, Science 351 (2016) 58–62, https://doi.org/10.1126/science.aad2688.
[96] J.F. Cawthray, D.M. Weekes, O. Sivak, A.L. Creagh, F. Ibrahim, M. Iafrate, C. A. Haynes, K.M. Wasan, C. Orvig, In vivo study and thermodynamic investigation of two lanthanum complexes, $La(Dpp)_3$ and La(XT), for the treatment of bone resorption disorders, Chem. Sci. 6 (2015) 6439–6447, https://doi.org/10.1039/c5sc01767j.
[97] J. Mintz, A. Vedenko, O. Rosete, K. Shah, G. Goldstein, J.M. Hare, R. Ramasamy, H. Arora, Current advances of nitric oxide in cancer and anticancer therapeutics, Vaccines 9 (2021) 94, https://doi.org/10.3390/vaccines9020094.
[98] T.L. Tan, H.M. Jin, M.B. Sullivan, B. Anasori, Y. Gogotsi, High-throughput survey of ordering configurations in MXene alloys across compositions and temperatures, ACS Nano 11 (2017) 4407–4418, https://doi.org/10.1021/acsnano.6b08227.
[99] R. Mohammadinejad, A. Dehshahri, V. Sagar Madamsetty, M. Zahmatkeshan, S. Tavakol, P. Makvandi, D. Khorsandi, A. Pardakhty, M. Ashrafizadeh, E. Ghasemipour Afshar, A. Zarrabi, *In vivo* gene delivery mediated by non-viral vectors for cancer therapy, J. Contr. Release 325 (2020) 249–275, https://doi.org/10.1016/j.jconrel.2020.06.038.
[100] R. Fu, H. Li, R. Li, K. McGrath, G. Dotti, Z. Gu, Delivery techniques for enhancing car T cell therapy against solid tumors, Adv. Funct. Mater. (2021) 2009489, https://doi.org/10.1002/adfm.202009489.
[101] Y. Shi, H. Inoue, J.C. Wu, S. Yamanaka, Induced pluripotent stem cell technology: a decade of progress, Nat. Rev. Drug Discov. 16 (2017) 115–130, https://doi.org/10.1038/nrd.2016.245.
[102] N.J. Yang, M.J. Hinner, Getting across the cell membrane: an overview for small molecules, peptides, and proteins, Methods Mol. Biol. 1266 (2015) 29–53, https://doi.org/10.1007/978-1-4939-2272-7_3.
[103] M.P. Stewart, A. Sharei, X. Ding, G. Sahay, R. Langer, K.F. Jensen, *In vitro* and *ex vivo* strategies for intracellular delivery, Nature 538 (2016) 183–192, https://doi.org/10.1038/nature19764.
[104] H.-X. Wang, M. Li, C.M. Lee, S. Chakraborty, H.-W. Kim, G. Bao, K.W. Leong, CRISPR/Cas9-Based genome editing for disease modeling and therapy: challenges and opportunities for nonviral delivery, Chem. Rev. 117 (2017) 9874–9906, https://doi.org/10.1021/acs.chemrev.6b00799.
[105] M.P. Stewart, R. Langer, K.F. Jensen, Intracellular delivery by membrane disruption: mechanisms, strategies, and concepts, Chem. Rev. 118 (2018) 7409–7531, https://doi.org/10.1021/acs.chemrev.7b00678.
[106] Y. Qu, Y. Zhang, Q. Yu, H. Chen, Surface-mediated intracellular delivery by physical membrane disruption, ACS Appl. Mater. Interfaces 12 (2020) 31054–31078, https://doi.org/10.1021/acsami.0c06978.
[107] R. Xiong, S.K. Samal, J. Demeester, A.G. Skirtach, S.C. De Smedt, K. Braeckmans, Laser-assisted photoporation: fundamentals, technological advances and applications, Adv. Phys. X 1 (2016) 596–620, https://doi.org/10.1080/23746149.2016.1228476.
[108] J.C. Fraire, G. Houthaeve, J. Liu, L. Raes, L. Vermeulen, S. Stremersch, T. Brans, G. Garcia-Diaz Barriga, S. De Keulenaer, F. Van Nieuwerburgh, R. De Rycke, J. Vandesompele, P. Mestdagh, K. Raemdonck, W.H. De Vos, S. De Smedt, K. Braeckmans, Vapor nanobubble is the more reliable photothermal mechanism for inducing endosomal escape of sirna without disturbing cell homeostasis, J. Contr. Release 319 (2020) 262–275, https://doi.org/10.1016/j.jconrel.2019.12.050.
[109] T.-H. Wu, S. Kalim, C. Callahan, M. Teitell, P.-Y. Chiou, Light image patterned molecular delivery into live, Opt Express 18 (2010) 938–946, https://doi.org/10.1109/leosst.2008.4590556.
[110] Z. Lyu, F. Zhou, Q. Liu, H. Xue, Q. Yu, H. Chen, A universal platform for macromolecular delivery into cells using gold nanoparticle layers via the photoporation effect, Adv. Funct. Mater. 26 (2016) 5787–5795, https://doi.org/10.1002/adfm.201602036.
[111] J. Wu, H. Xue, Z. Lyu, Z. Li, Y. Qu, Y. Xu, L. Wang, Q. Yu, H. Chen, Intracellular delivery platform for "recalcitrant" cells: when polymeric carrier marries photoporation, ACS Appl. Mater. Interfaces 9 (2017) 21593–21598, https://doi.org/10.1021/acsami.7b06201.
[112] J. Wang, K.-F. Ren, Y.-F. Gao, H. Zhang, W.-P. Huang, H.-L. Qian, Z.-K. Xu, J. Ji, Photothermal spongy film for enhanced surface-mediated transfection to primary cells, ACS Appl. Bio Mater. 2 (2019) 2676–2684, https://doi.org/10.1021/acsabm.9b00358.

[113] H. Zhang, J. Wang, M. Hu, B.-c. Li, H. Li, T.-t. Chen, K.-F. Ren, J. Ji, Q.-m. Jing, G.-s. Fu, Photothermal-assisted surface-mediated gene delivery for enhancing transfection efficiency, Biomater. Sci. 7 (2019) 5177–5186, https://doi.org/10.1039/C9BM01284B.
[114] L. Wang, J. Wu, Y. Hu, C. Hu, Y. Pan, Q. Yu, H. Chen, Using porous magnetic iron oxide nanomaterials as a facile photoporation nanoplatform for macromolecular delivery, J. Mater. Chem. B 6 (2018) 4427–4436, https://doi.org/10.1039/c8tb01026a.
[115] J. Wu, Y. Zheng, S. Jiang, Y. Qu, T. Wei, W. Zhan, L. Wang, Q. Yu, H. Chen, Two-in-One platform for high-efficiency intracellular delivery and cell harvest: when a photothermal agent meets a thermoresponsive polymer, ACS Appl. Mater. Interfaces 11 (2019) 12357–12366, https://doi.org/10.1021/acsami.9b01586.
[116] T.H. Kang, S. Lee, J.A. Kwon, J. Song, I. Choi, Photothermally enhanced molecular delivery and cellular positioning on patterned plasmonic interfaces, ACS Appl. Mater. Interfaces 11 (2019) 36420–36427, https://doi.org/10.1021/acsami.9b13576.
[117] Y. Zheng, Y. Wu, Y. Zhou, J. Wu, X. Wang, Y. Qu, Y. Wang, Y. Zhang, Q. Yu, Photothermally activated electrospun nanofiber mats for high-efficiency surface-mediated gene transfection, ACS Appl. Mater. Interfaces 12 (2020) 7905–7914, https://doi.org/10.1021/acsami.9b20221.
[118] S. Courvoisier, N. Saklayen, M. Huber, J. Chen, E.D. Diebold, L. Bonacina, J. P. Wolf, E. Mazur, Plasmonic tipless pyramid arrays for cell poration, Nano Lett. 15 (2015) 4461–4466, https://doi.org/10.1021/acs.nanolett.5b01697.
[119] N. Saklayen, M. Huber, M. Madrid, V. Nuzzo, D.I. Vulis, W. Shen, J. Nelson, A. A. McClelland, A. Heisterkamp, E. Mazur, Intracellular delivery using nanosecond-laser excitation of large-area plasmonic substrates, ACS Nano 11 (2017) 3671–3680, https://doi.org/10.1021/acsnano.6b08162.
[120] A. Raun, N. Saklayen, C. Zgrabik, W. Shen, M. Madrid, M. Huber, E. Hu, E. Mazur, A comparison of inverted and upright laser-activated titanium nitride micropyramids for intracellular delivery, Sci. Rep. 8 (2018) 15595, https://doi.org/10.1038/s41598-018-33885-y.
[121] T. Man, X. Zhu, Y.T. Chow, E.R. Dawson, X. Wen, A.N. Patananan, T.L. Liu, C. Zhao, C. Wu, J.S. Hong, P.S. Chung, D.L. Clemens, B.Y. Lee, P.S. Weiss, M. A. Teitell, P.Y. Chiou, Intracellular photothermal delivery for suspension cells using sharp nanoscale tips in microwells, ACS Nano 13 (2019) 10835–10844, https://doi.org/10.1021/acsnano.9b06025.
[122] C. Zhao, T. Man, X. Xu, Q. Yang, W. Liu, S.J. Jonas, M.A. Teitell, P.-Y. Chiou, P. S. Weiss, Photothermal intracellular delivery using gold nanodisk arrays, ACS Mater. Lett. 2 (2020) 1475–1483, https://doi.org/10.1021/acsmaterialslett.0c00428.
[123] G.C. Messina, M. Dipalo, R. La Rocca, P. Zilio, V. Caprettini, R. Proietti Zaccaria, A. Toma, F. Tantussi, L. Berdondini, F. De Angelis, Spatially, temporally, and quantitatively controlled delivery of broad range of molecules into selected cells through plasmonic nanotubes, Adv. Mater. 27 (2015) 7145–7149, https://doi.org/10.1002/adma.201503252.
[124] Y.C. Wu, T.H. Wu, D.L. Clemens, B.Y. Lee, X. Wen, M.A. Horwitz, M.A. Teitell, P. Y. Chiou, Massively parallel delivery of large cargo into mammalian cells with light pulses, Nat. Methods 12 (2015) 439–444, https://doi.org/10.1038/nmeth.3357.
[125] Y. Qu, Y. Zheng, L. Yu, Y. Zhou, Y. Wang, Y. Zhang, Q. Yu, H. Chen, A universal platform for high-efficiency "engineering" living cells: integration of cell capture, intracellular delivery of biomolecules, and cell harvesting functions, Adv. Funct. Mater. 30 (2020) 1906362, https://doi.org/10.1002/adfm.201906362.
[126] S. Yang, C. Zhou, J. Liu, Editorial:The golden era: gold nanomaterials for bioapplications, Front. Chem. 8 (2020) 780, https://doi.org/10.3389/fchem.2020.00780.
[127] J. Wu, Y. Qu, Q. Yu, H. Chen, Gold nanoparticle layer: a versatile nanostructured platform for biomedical applications, Mater. Chem. Front. 2 (2018) 2175–2190, https://doi.org/10.1039/C8QM00449H.
[128] Y. Qu, T. Wei, J. Zhao, S. Jiang, P. Yang, Q. Yu, H. Chen, Regenerable smart antibacterial surfaces: full removal of killed bacteria via a sequential degradable layer, J. Mater. Chem. B 6 (2018) 3946–3955, https://doi.org/10.1039/C8TB01122B.
[129] R. Mrowczynski, Polydopamine-based multifunctional (nano) materials for cancer therapy, ACS Appl. Mater. Interfaces 10 (2018) 7541–7561, https://doi.org/10.1021/acsami.7b08392.
[130] H.A. Lee, Y. Ma, F. Zhou, S. Hong, H. Lee, Material-independent surface chemistry beyond polydopamine coating, Acc. Chem. Res. 52 (2019) 704–713, https://doi.org/10.1021/acs.accounts.8b00583.
[131] R.H. Buckley, Transplantation of hematopoietic stem cells in human severe combined immunodeficiency: longterm outcomes, Immunol. Res. 49 (2011) 25–43, https://doi.org/10.1007/s12026-010-8191-9.
[132] J. Kobayashi, M. Yamato, T. Okano, On-off affinity binding modulation on thermoresponsive polymer-grafted surfaces for capture and release of proteins and cells, J. Biomater. Sci. Polym. Ed. 28 (2017) 939–957, https://doi.org/10.1080/09205063.2017.1295508.
[133] M. Ullah, A. Wahab, D. Khan, S. Saeed, S.U. Khan, N. Ullah, T.A. Saleh, Modified gold and polymeric gold nanostructures: toxicology and biomedical applications, Colloid Interface Sci. Commun. 42 (2021) 100412, https://doi.org/10.1016/j.colcom.2021.100412.
[134] Y. Pan, S. Neuss, A. Leifert, M. Fischler, F. Wen, U. Simon, G. Schmid, W. Brandau, W. Jahnen-Dechent, Size-dependent cytotoxicity of gold nanoparticles, Small 3 (2007) 1941–1949, https://doi.org/10.1002/smll.200700378.
[135] S. Mizrahy, I. Hazan-Halevy, N. Dammes, D. Landesman-Milo, D. Peer, Current progress in non-viral RNAi-based delivery strategies to lymphocytes, Mol. Ther. 25 (2017) 1491–1500, https://doi.org/10.1016/j.ymthe.2017.03.001.
[136] J. Wang, Y. Wei, S. Zhao, Y. Zhou, W. He, Y. Zhang, W. Deng, The analysis of viability for mammalian cells treated at different temperatures and its application in cell shipment, PloS One 12 (2017), https://doi.org/10.1371/journal.pone.0176120 e0176120.
[137] Q. Yu, H. Liu, H. Chen, Vertical sinwas for biomedical and biotechnology applications, J. Mater. Chem. B 2 (2014) 7849–7860, https://doi.org/10.1039/c4tb01246a.
[138] Y. Zhou, Y. Zheng, T. Wei, Y. Qu, Y. Wang, W. Zhan, Y. Zhang, G. Pan, D. Li, Q. Yu, H. Chen, Multistimulus responsive biointerfaces with switchable bioadhesion and surface functions, ACS Appl. Mater. Interfaces 12 (2020) 5447–5455, https://doi.org/10.1021/acsami.9b18505.
[139] B.S. Gomes, B. Simões, P.M. Mendes, The increasing dynamic, functional complexity of bio-interface materials, Nat. Rev. Chem. 2 (2018), https://doi.org/10.1038/s41570-018-0120, 0120.
[140] L. Liu, X. Tian, Y. Ma, Y. Duan, X. Zhao, G. Pan, A versatile dynamic mussel-inspired biointerface: from specific cell behavior modulation to selective cell isolation, Angew. Chem. Int. Ed. 57 (2018) 7878–7882, https://doi.org/10.1002/anie.201804802.
[141] X. Zhao, L. Jin, H. Shi, W. Tong, D. Gorin, Y. Kotelevtsev, Z. Mao, Recent advances of designing dynamic surfaces to regulate cell adhesion, Colloid Interface Sci. Commun. 35 (2020) 100249, https://doi.org/10.1016/j.colcom.2020.100249.
[142] H. Liu, X. Liu, J. Meng, P. Zhang, G. Yang, B. Su, K. Sun, L. Chen, D. Han, S. Wang, L. Jiang, Hydrophobic interaction-mediated capture and release of cancer cells on thermoresponsive nanostructured surfaces, Adv. Mater. 25 (2013) 922–927, https://doi.org/10.1002/adma.201203826.
[143] H. Liu, S. Wang, Poly(N-Isopropylacrylamide)-Based thermo-responsive surfaces with controllable cell adhesion, Sci. China Chem. 57 (2014) 552–557, https://doi.org/10.1007/s11426-013-5051-1.
[144] W. Li, J. Wang, J. Ren, X. Qu, Near-infrared- and pH-responsive system for reversible cell adhesion using graphene/gold nanorods functionalized with i-motif DNA, Angew. Chem. Int. Ed. 52 (2013) 6726–6730, https://doi.org/10.1002/anie.201302048.
[145] J. You, J.S. Heo, J. Kim, T. Park, B. Kim, H.-S. Kim, Y. Choi, H.O. Kim, E. Kim, Noninvasive photodetachment of stem cells on tunable conductive polymer nano thin films: selective harvesting and preserved differentiation capacity, ACS Nano 7 (2013) 4119–4128, https://doi.org/10.1021/nn400405t.
[146] J.J. Giner-Casares, M. Henriksen-Lacey, I. García, L.M. Liz-Marzán, Plasmonic surfaces for cell growth and retrieval triggered by near-infrared light, Angew. Chem. Int. Ed. 55 (2016) 974–978, https://doi.org/10.1002/anie.201509025.
[147] H. Cui, P. Zhang, W. Wang, G. Li, Y. Hao, L. Wang, S. Wang, Near-infrared (NIR) controlled reversible cell adhesion on a responsive nano-biointerface, Nano Res. 10 (2017) 1345–1355, https://doi.org/10.1007/s12274-017-1446-1.
[148] G.A. Vinnacombe-Willson, N. Chiang, L. Scarabelli, Y. Hu, L.K. Heidenreich, X. Li, Y. Gong, D.T. Inouye, T.S. Fisher, P.S. Weiss, S.J. Jonas, In situ shape control of thermoplasmonic gold nanostars on oxide substrates for hyperthermia-mediated cell detachment, ACS Cent. Sci. 6 (2020) 2105–2116, https://doi.org/10.1021/acscentsci.0c01097.
[149] S.-W. Lv, Y. Liu, M. Xie, J. Wang, X.-W. Yan, Z. Li, W.-G. Dong, W.-H. Huang, Near-infrared light-responsive hydrogel for specific recognition and photothermal site-release of circulating tumor cells, ACS Nano 10 (2016) 6201–6210, https://doi.org/10.1021/acsnano.6b02208.
[150] X. Wang, X. Wang, S. Cheng, M. Ye, C. Zhang, Y. Xian, Near-infrared light-switched MoS_2 Nanoflakes@Gelatin bioplatform for capture, detection, and nondestructive release of circulating tumor cells, Anal. Chem. 92 (2020) 3111–3117, https://doi.org/10.1021/acs.analchem.9b04724.
[151] J.D. Kim, J.S. Heo, T. Park, C. Park, H.O. Kim, E. Kim, Photothermally induced local dissociation of collagens for harvesting of cell sheets, Angew. Chem. Int. Ed. 54 (2015) 5869–5873, https://doi.org/10.1002/anie.201411386.
[152] J. Na, J.S. Heo, M. Han, H. Lim, H.O. Kim, E. Kim, Harvesting of living cell sheets by the dynamic generation of diffractive photothermal pattern on PEDOT, Adv. Funct. Mater. 27 (2017) 1604260, https://doi.org/10.1002/adfm.201604260.
[153] J. Na, S.Y. Song, J.D. Kim, M. Han, J.S. Heo, C.E. Yang, H.O. Kim, D.H. Lew, E. Kim, Protein-engineered large area adipose-derived stem cell sheets for wound healing, Sci. Rep. 8 (2018) 15869, https://doi.org/10.1038/s41598-018-34119-x.
[154] J. Jing, S. Chen, Q. Lu, Gradient photothermal field for precisely directing cell sheet detachment, Adv. Biosys. 3 (2019) 1800334, https://doi.org/10.1002/adbi.201800334.
[155] J.-F. Lutz, Thermo-switchable materials prepared using the OEGMA-platform, Adv. Mater. 23 (2011) 2237–2243, https://doi.org/10.1002/adma.201100597.
[156] C. Weber, R. Hoogenboom, U.S. Schubert, Temperature responsive bio-compatible polymers based on poly(ethylene oxide) and poly(2-oxazoline)s, Prog. Polym. Sci. 37 (2012) 686–714, https://doi.org/10.1016/j.progpolymsci.2011.10.002.
[157] G. Chen, Y. Qi, L. Niu, T. Di, J. Zhong, T. Fang, W. Yan, Application of the cell sheet technique in tissue engineering, *biomed*, For. Rep. 3 (2015) 749–757, https://doi.org/10.3892/br.2015.522.
[158] M. Li, J. Ma, Y. Gao, L. Yang, Cell sheet technology: a promising strategy in regenerative medicine, Cytotherapy 21 (2019) 3–16, https://doi.org/10.1016/j.jcyt.2018.10.013.
[159] T. Owaki, T. Shimizu, M. Yamato, T. Okano, Cell sheet engineering for regenerative medicine: current challenges and strategies, Biotechnol. J. 9 (2014) 904–914, https://doi.org/10.1002/biot.201300432.
[160] K. Mokhtarinia, M.S. Nourbakhsh, E. Masaeli, M. Entezam, F. Karamali, M. H. Nasr-Esfahani, Switchable phase transition behavior of thermoresponsive substrates for cell sheet engineering, J. Polym. Sci. 56 (2018) 1567–1576, https://doi.org/10.1002/polb.24744.

[161] J. Baek, Y. Cho, H.J. Park, G. Choi, J.S. Lee, M. Lee, S.J. Yu, S.W. Cho, E. Lee, S. G. Im, A surface-tailoring method for rapid non-thermosensitive cell-sheet engineering via functional polymer coatings, Adv. Mater. 32 (2020) 1907225, https://doi.org/10.1002/adma.201907225.

[162] H. Chen, K. Shou, S. Chen, C. Qu, Z. Wang, L. Jiang, M. Zhu, B. Ding, K. Qian, A. Ji, H. Lou, L. Tong, A. Hsu, Y. Wang, D.W. Felsher, Z. Hu, J. Tian, Z. Cheng, Smart self-assembly amphiphilic cyclopeptide-dye for near-infrared window-II imaging, Adv. Mater. 33 (2021) 2006902, https://doi.org/10.1002/adma.202006902.

[163] J. Li, X. Yu, Y. Jiang, S. He, Y. Zhang, Y. Luo, K. Pu, Second near-infrared photothermal semiconducting polymer nanoadjuvant for enhanced cancer immunotherapy, Adv. Mater. 33 (2021) 2003458, https://doi.org/10.1002/adma.202003458.

[164] S. Wang, X. Li, S.Y. Chong, X. Wang, H. Chen, C. Chen, L.G. Ng, J.W. Wang, B. Liu, In vivo three-photon imaging of lipids using ultrabright fluorogens with aggregation-induced emission, Adv. Mater. 33 (2021) 2007490, https://doi.org/10.1002/adma.202007490.